

Seasonal variation in chemical composition of size-segregated aerosols over the Northeastern Arabian Sea

Ankush Kaushik¹, Ashwini Kumar^{1*}, Aswini M. A¹, Panda, P. P.¹, Garima Shukla^{1,2}, N.C. Gupta³

¹CSIR-National Institute of Oceanography, Dona Paula, Goa, India

²Academy of Scientific and Innovative Research (AcSIR), CSIR-National Institute of Oceanography, Goa, India

³Guru Gobind Singh Indraprastha University, Dwarka Sector-16C, New Delhi, India

***Corresponding author:** Ashwini Kumar, Geological Oceanography Division
CSIR-National Institute of Oceanography
Dona Paula, Goa-403 004
E-mail: ashwinikumarjha@gmail.com,
ashwinik@nio.org
Tel: +91 832 2450368, Fax: +91 832 2450602

Abstract:

Water-soluble species constitute a significant fraction (up to 60 – 70 %) of the total aerosol loading in the marine atmospheric boundary layer (MABL). The “indirect” effects i.e. climate forcing due to modification of cloud properties depend on the water-soluble composition of aerosols. Thus, the characterization of aerosols over the MABL is of greater relevance. Here, we present, 1-year long aerosol chemical composition data of PM₁₀ and PM_{2.5} at a costal location in the Northeastern Arabian Sea (Goa; 15.46°N, 73.8°E, 56 m above the sea level). Average water-soluble ionic concentration (sum of anion and cation) are highest ($25.5 \pm 6.9 \mu\text{g m}^{-3}$ and $19.6 \pm 5.8 \mu\text{g m}^{-3}$ for PM₁₀ and PM_{2.5} respectively) during winter season and lowest during post-monsoon (17.3 ± 9.1 and $14.4 \pm 8.1 \mu\text{g m}^{-3}$ for PM₁₀ and PM_{2.5} respectively). Among water-soluble ionic species, SO₄²⁻ ion was found to be dominant species in anions and NH₄⁺ is dominant in cations, for both PM₁₀ and PM_{2.5} during all the seasons. These observations clearly hints to the contribution from anthropogenic emission and significant secondary inorganic species formation. Sea-salt (calculated based on Na⁺ and Cl⁻) concentration shows significant temporal variability with highest contribution during summer seasons in both fractions. Sea-salt corrected Ca²⁺, an indicator of mineral dust is found mostly during summer months, particularly in PM₁₀ samples, indicate contribution from mineral dust emissions from arid/semi-arid regions located in the north/northwestern India and South west Asia. These observations are corroborated with back-trajectory analyses, wherein, air-parcels were found to derive from Desert area in summer and Indo-Gangetic Plains (a hot-spot for anthropogenic emissions) during winter. In addition, we also observe, presence of nss-K⁺ (sea-salt corrected), for PM_{2.5}, particularly during winter months, indicating influence of biomass burning emissions. The impact on aerosol chemistry is further assessed based on chloride depletion. Chloride depletion is observed very significant during post-monsoon months (October and November), wherein, more than 80 % upto 100 % depletion is found, mediated by excess sulphates highlighting the role of secondary species in atmospheric chemistry. Regional scale characterization of atmospheric aerosols are important for their better parameterization in chemical transport model and estimation of radiative forcing.

Key words: Aerosols; Chemical composition; Arabian Sea; Water soluble ionic composition, Secondary inorganic species.

1. Introduction:

Atmospheric aerosols, derived from continental regions undergo long-range transport and supply significant amount of nutrients as well as toxicants to remote and coastal oceanic region (; Jickells et al., 2005; Paytan et al., 2009; Kumar et al., 2010; Jordi et al., 2012; Baker et al., 2013; Srinivas and Sarin, 2013a;;; Powell et al., 2015; Kumar et al., 2020). In addition, aerosols emitted from marine region (mainly sea-salt), can impact on the chemical composition of aerosols over the continent and, thus, play a vital role in atmospheric chemistry (Quinn et al., 2004; Keene et al., 2007; Kumar and Sarin, 2009; Sarin et al., 2011). The availability (and lability) of nutrients/toxicants significantly depend on the ambient atmospheric chemistry (Baker and Croot, 2010; Kumar et al., 2010a), which eventually undergo dry (Arimoto et al., 2003; Srinivas and Sarin, 2013a; Baker et al., 2017) as well as wet (Measures and Vink, 1999; Chance et al., 2015; Powell et al., 2015;) deposition. Post deposition, they can modulate surface water biogeochemical processes (Mahowald et al., 2005; Guieu et al., 2019; Anderson, 2020; ;) which have impact on carbon cycling and eventually on Earth's climate (Ramanathan et al., 2001; Barnett et al., 2005; Rana et al., 2019).

The lifetime of atmospheric aerosols ranges from few hours to several days, and thus, they display large temporal variability (Pöschl, 2005). In addition, varying emission intensity and their source region also contribute to their temporal as well as spatial variability. The impact of aerosols can be assessed more quantitatively by having information on their chemical composition as well as their emission sources. For example, aerosols with more acidic composition have more processed labile Fe content (Baker and Croot, 2010; Kumar et al., 2010) and can impact significantly on primary productivity of the oceanic region where it will be deposited. Similarly, aerosols characterized with enriched Fe/Al ratio (Kumar and Sarin, 2010a; Srinivas and Sarin, 2013a, b) will supply more Fe which can contribute to enhanced primary productivity. Furthermore, the abundances and atmospheric reactivity of acidic species (nitrate and sulphate) largely depend on the size distribution (Sullivan et al., 2007), which have potential to enhance the bioavailability of nutrients (Baker and Croot, 2010; Kumar et al., 2010a). Thus, one of the major limitations of current models relates to the lack of data on size dependent chemical composition of atmospheric aerosols and the associated spatio-temporal variability. Considering the importance of chemical composition, efforts have been made in the past to chemically characterize aerosols over continental (Wang and Shooter, 2001; Tare et al., 2006; Williams et al., 2007; Ng et al., 2011; Sahai et al., 2011; Sun et al., 2012; Jain et al., 2014; Tiwari et al., 2014; Petit et al., 2015;) as well as marine regions (Siefert et al., 1999; Johansen and Hoffmann, 2003; Kumar et al., 2008a, 2008b; van Pinxteren et al., 2015; Budhavant et al., 2017; Pan et al., 2018; Aswini et al., 2020a; Cvitešić Kušan et al., 2020;).

Owing to high population density and rapid industrialization, Indian subcontinent is considered as one of the major hotspots for anthropogenic emissions (Streets et al., 2003; Srivastava et al., 2012; Tiwari et al., 2014; Sen et al., 2017; Ningombam et al., 2020; Ojha et al., 2020) which further make the adjoining marine region vulnerable to these emissions (Kumar et al., 2010a, 2010b; Srinivas and Sarin, 2013b; Srinivas et al. 2019; Rastogi et al., 2020). In view of this, several field observations, long term (Williams et al., 2007; Kumar and Sarin, 2009; Jain et al., 2014; Tiwari et al., 2014; Kishore et al., 2019;) and campaign based (Venkataraman et al., 2002; Kumar et al., 2008a, 2008b; Sahai et al., 2011; Aswini et al., 2020a) as well as remote sensing (Woo et al., 2003; Venkataraman et al., 2006; Srivastava et al., 2012; Mehta et al., 2016; Sen et al., 2017; Thomas et al., 2019;) and modelling studies (Pant and Harrison, 2012; Michael et al., 2013, 2014; Moorthy et al., 2013; Govardhan et al., 2015; Mukherjee et al., 2018;) have been reported from India to understand chemical and physical properties of aerosols. However, major focus have been so far on the urban (Rastogi and Sarin, 2005; Jain et al., 2014; Tiwari et al., 2014; Sharma et al., 2016; Budhavant et al., 2017; Kishore et al., 2019;;) rural (Lawrence and Taneja 2005; Balakrishnan et al. 2018; Gautam et al. 2020;) and remote high altitude (Shrestha et al., 1997; Chatterjee et al., 2010; Kumar and Sarin, 2010b; Saxena et al., 2016; Gautam et al., 2018; Ganguly et al., 2019;) locations, leaving a large scope for studies on aerosol chemical composition near and/or over the marine region adjoining Indian subcontinent. There have been very limited studies reported from coastal locations around India (Madhavan et al., 2008; Agnihotri et al., 2015; Aswini et al., 2020a; Yadav et al., 2020), which are mainly based on the bulk composition and provide a snapshot picture of aerosols composition. Recently, Thomas et al., 2019, have highlighted an increasing trend of aerosol optical depth over the coastal Arabian Sea compared to the Bay of Bengal during winter months. These observations further suggest the need for long term field based observations of chemical composition of aerosols over the coastal Arabian Sea.

Here we report a comprehensive data set on chemical composition of PM₁₀ and PM_{2.5} collected for around one year at a coastal location in the northeaster Arabian Sea. Our main objective is to assess seasonal variability of chemical constituents in PM₁₀ and PM_{2.5} and to identify major sources impacting aerosol composition at the study site. In addition, we have also assessed the role of various chemical processes impacting on the chemical composition of ambient aerosols collected at our study site. Our detailed study involving use of chemical constituents and their ratios as diagnostic tracers, in conjunction with meteorological parameters, is an important contribution towards understanding of surface water biogeochemical processes operative in the coastal Arabian Sea.

2. Materials and methodology:

2.1 Study area:

The observational site is located (Fig. 1) at Goa (15.45°N, 73.20°E) on the west coast of India in the campus of CSIR-National Institute of Oceanography (CSIR-NIO). The sampling location is surrounded by the Arabian Sea on the west and Western Ghats on the eastern side (Aswini et al., 2020b; Kumar et al., 2020). Being in the tropical zone and near the Arabian Sea, Goa has a warm, humid climate for most of the year. Sampling site is 500 m away from the Arabian Sea and also can be considered as a representative site for the Northeastern Arabian Sea (Kumar et al. 2020)

2.2 Methodology:

Atmospheric aerosols with 50% cut off aerodynamic diameter of 10 microns (PM₁₀) and 2.5 micron (PM_{2.5}) were collected on PALLFLEX™ Tissuquartz filters (8" x 10") by using high-volume sampler (TISCH Environmental) at an average flow rate of 1.1 m³min⁻¹. Few samples, between April-2018 and May-2018, were collected on Whatman-41 rectangular cellulose filters (20cm x 25cm) using same high-volume samplers. The sampler was set up on the terrace (15.45°N, 73.20°E) of NIO building at the height of 56 m from ground level. Typically, each sample was collected by operating the sampler for 24-hours with a sampling frequency of 2 samples per week. A total of 224 PM₁₀ and PM_{2.5} samples (more details are in Table-1) were collected from December 2017 to February 2019. Prior to sample collection, quartz filters were conditioned in an oven at a temperature of 200 °C for 3-4 hours.

A piece (1/8th) of filter sample was cut from the sampled area using ceramic scissor under clean laminar flow bench. This filter piece along with deionized water (Milli-Q; specific resistivity >18.2 MΩ-cm) was transferred into 50 mL Savillex bombs and subjected to ultra-sonication for 30 min. The water extracts were subsequently filtered through a PVDF syringe filter with pore size 0.2 μm and then transferred to a pre-conditioned polypropylene bottle. This filtered solution was analysed for cations (Na⁺, NH₄⁺, K⁺, Mg²⁺ and Ca²⁺) and anions (Cl⁻, NO₃⁻ and SO₄²⁻) using Thermo Scientific Ion Chromatography System (Dionex ICS 5000). The cations (Na⁺, NH₄⁺, K⁺, Mg²⁺ and Ca²⁺) were analysed using the analytical column Ion Pac CS12A, 4 × 250 mm and guard column Ion Pac CG12A, 4 × 50 mm using CSRS 300 as a suppressor. Methyl sulphonic acid has been used as an eluent for the cation analysis with a run time of 15 minutes. The anions (Cl⁻, NO₃⁻ and SO₄²⁻) were analysed using the analytical column Ion Pac AS16, 4 × 250 mm and guard column Ion Pac AG16, 4 × 50 mm using ASRS 300 as suppressor. 22mM NaOH Solution has been used as eluent for the anion analysis with the run time of 10 minutes. Merck multi elements standard was used for standard preparation by suitably diluting it. Daily calibrations were done before starting the analyses and fresh standards were

prepared before analyses. Along with samples, field blanks were also extracted and analysed using similar methodology as that of aerosol samples. The concentrations of ionic species were corrected for procedural blanks. Based on blank concentrations and average volume of air filtered ($\sim 2000 \text{ m}^3$), the detection limits for the water-soluble ionic species in aerosols were ascertained (18, 18, 20, 18, 25, 10, 30 and 30 ng m^{-3} for Na^+ , NH_4^+ , K^+ , Mg^{2+} , Ca^{2+} , Cl^- , NO_3^- and SO_4^{2-} respectively). The reproducibility in the analytical data for the measured concentrations is within 5% based on the repeat analysis of a number of samples and standards.

Meteorological data were obtained using Automatic Weather System (AWS) installed at the roof top ($\sim 56 \text{ m}$ above the sea level) of the CSIR-National Institute of Oceanography (details of AWS are given in Mehra et al., 2005). In our study, we classified three different seasons (1) Winter (WIN) during December-February; (2) Summer (SUM) during March-May and (3) Post-monsoon (POM) during September-November, based on the previous studies (Agnihotri et al., 2015; Yadav et al., 2020) at this site. Using this classification, we computed 7-days air mass back trajectory (AMBT) ending at our study site for each sampling day (Fig. 2). The AMBTs were computed using HYSPLIT-4 model and GDAS dataset of National Oceanic and Atmospheric Administration Air Resource Laboratory (NOAA) at 500 m altitude (Stein et al., 2015). Fig. S1 and S2 depict the seasonal variation of temperature, relative humidity (RH) respectively. In winter the average temperature was found to be $25 \text{ }^\circ\text{C}$ with average RH 72%, in summer average temperature was $28 \text{ }^\circ\text{C}$ with average RH 82% and during post-monsoon average recorded temperature was $26 \text{ }^\circ\text{C}$ with average RH 90%. Although, we did not observe significant variation in temperature and relative humidity during different seasons, however, significant changes in wind trajectories were observed and discussed in detail in the next section.

3. Results and Discussions:

3.1 Back trajectory analyses:

The AMBTs corresponding to different seasons, for sample collection days, are shown in Fig. 2 with different colours. A distinct wind pattern is observed for WIN and SUM months; however, mixed winds are seen during POM season. Winds are mostly derived from marine region as well as Middle-east deserts during SUM seasons, with several trajectories crossing over the coastal region of Western India, Pakistan and Iran-Pakistan border region. In contrast, winds during WIN season, are mostly derived from continental locations in Indian subcontinent, particularly from the Indo-Gangetic Plains (one of the hotspots for anthropogenic emissions during WIN; Thomas et al., 2019). Those derived during WIN are also observed to pass over the coastal region of eastern India as well as over

the Bay of Bengal (Fig. 2). After the southwest monsoon withdrawal, winds origin is observed from marine as well as continental locations, with few winds derived from coastal northwest Africa and far eastern part of the Bay of Bengal. In order to identify major contribution from emission sources during POM, we have done cluster analyses (Stein et al., 2015) all AMBTs computed during this period. Our analyses indicate the dominance of continental sources (more than 65 %) as compared to marine sources (Fig. S3). It is interesting to note here that majority of winds at our study site indicate long-range transport trajectories possibly bringing aerosols derived from variety of sources including natural arid/semi-arid desert and marine regions as well as polluted anthropogenic locations. Thus, it is apparent, meteorology may play an important role in impacting ambient aerosol composition leading to a strong seasonal variability at this location.

3.2. Seasonal variability of water-soluble ionic composition in PM₁₀ and PM_{2.5}:

In this study, a total of 224 aerosol samples were collected, which includes 112 PM₁₀ and 112 PM_{2.5} samples (detail of number of samples, sampling days in each month and type of filter used for PM collection is tabulated in Table-1). Water soluble ionic composition (WSIC) is calculated by adding mass concentration ($\mu\text{g m}^{-3}$) of all cations (Na^+ , NH_4^+ , K^+ , Mg^{2+} and Ca^{2+}) and anions (Cl^- , NO_3^- and SO_4^{2-}) measured in this study. The charge balance (in equivalent units) between total cations (Σ^+) and total anions (Σ^-) is used to assess reliability and quality of the WSIC data (Kumar et al., 2008a, b). A correlation plot between Σ^+ and Σ^- is shown in Fig. 3, wherein, we observe most of the data are falling on or near to the 1:1 line for both PM₁₀ and PM_{2.5} samples. We observe, significant correlation between Σ^+ and Σ^- for all PM₁₀ and PM_{2.5} samples (r^2 is shown in Fig. 3), except for some PM₁₀ and PM_{2.5} (Fig. 3) samples, particularly during SUM months. The equivalence ionic ratio (Σ^-/Σ^+) for PM₁₀ varied from, 0.80 to 1.18 (mean: 1.00 ± 0.07) in WIN, 0.69 to 1.48 (mean: 0.99 ± 0.11) in SUM and 0.91 to 1.26 (mean: 1.06 ± 0.07) in POM seasons. PM_{2.5} samples shows similar ratios ranging from 0.82 to 1.20 (mean: 0.98 ± 0.07), 0.64 to 1.16 (mean 0.97 ± 0.11), and 0.80 to 1.19 (mean: 1.01 ± 0.11) during WIN, SUM and POM season respectively. We observed some of the SUM samples (PM₁₀ and PM_{2.5}) are falling away from the 1:1 line towards cation axis. Such deviation indicates anion deficit which can be attributed to the lack of measurement of bicarbonate ions which are mainly contributed by alkaline dust (Kumar et al., 2008a). The wind trajectories during SUM are mostly derived from the arid/semi-arid desert region which can potentially bring mineral dust to our sampling site. Similar anion deficit has been reported by (Kumar et al., 2008b) over the Bay of Bengal region during March-April, 2006. In addition, several studies have suggested lack of measurement of organic anions which can contribute to the anion budget of ambient aerosols (Kulshrestha et al 1998; Momin et al 1999; Venkatraman et al 2002; Rastogi and Sarin 2005).

The seasonal variation of WSIC mass concentration for PM₁₀ and PM_{2.5} are shown in Fig. 4 using Box-whisker plot. WSIC concentration is found to be highest for WIN samples in PM₁₀ (mean: 25.5±6.9; range: 10.4-50.0 µg m⁻³) followed by SUM (mean: 21.0±4.6; range: 12.8-30.4 µg m⁻³) and POM (mean: 17.3±9.1; range: 6.9-41.1 µg m⁻³) seasons. Similarly, WSIC in PM_{2.5} is high for WIN (mean: 19.6±5.8; range: 10.1-39.9 µg m⁻³), however, is relatively higher during POM (mean: 14.4±8.0; range: 2.3-29.0 µg m⁻³) as compared to SUM (mean: 12.9±7.3; range: 0.8-31.6 µg m⁻³) months. Compared to WIN and SUM, we observed large variability in WSIC during POM months, suggesting significant variability in sources, which is also supported by variation in AMBTs (Fig. 2) during this period. Agnihotri et al., (2015), have reported on bulk aerosol chemical composition for WIN and SUM months during 2009-2011, wherein they observed high WSIC during SUM compared to WIN months. Another study by Yadav et al. (2020), have also observed higher WSIC for SUM than that in WIN for total suspended particulate (TSP or bulk) aerosol samples. However, they observed high WSIC in WIN compared to SUM for PM₁₀ and PM_{2.5} samples during the year 2013 similar to our observation. The presence of sea-salts, which are abundant in coarser fraction, contribute more during SUM (also supported by AMBTs) in the bulk samples, as our sampling site is very near to coast. These coarser sea-salts are relatively less collected on filters, while sampling using PM₁₀ and PM_{2.5} inlets, as compared to bulk sampling. Thus, we (and previous studies) have observed higher WSIC for bulk during SUM compared to those collected with inlet of lower cut-off aerodynamic diameter.

In order to assess the relative contribution of PM_{2.5}-WSIC to PM₁₀-WSIC, a scatter plot between PM₁₀ and PM_{2.5} WSIC is shown in Fig. 5 for all three seasons. It is evident that majority of SUM samples are falling away from the 1:1 line towards the PM₁₀ axis, however, POM and WIN samples are relatively near and/or on the 1:1 line. This suggest, dominant contribution of fine mode WSIC towards water soluble composition of PM₁₀ during WIN and POM months. However, during summer months, PM₁₀ mass could be dominated by coarser sea-salt and mineral dust particles (more detail on their abundance in different size fraction is discussed in later section), which contribute relatively less to the PM_{2.5} mass. This is also evident from the ratio of WSIC-PM_{2.5}/WSIC-PM₁₀, which is found to be relatively low (0.59±0.24) during SUM compared to WIN (0.78±0.14) and POM (0.76±0.18) months. Our observation is consistent with those reported by (Agnihotri et al., 2015), which highlighted predominance of the sea-salt and mineral dust during SUM months compared to WIN season.

The percentage contribution of an individual water-soluble species to the total WSIC (of PM₁₀ and PM_{2.5}) is represented as pie-charts (Fig. 6) for the three different seasons. Sulphate (SO₄²⁻) and ammonium (NH₄⁺) ions, are dominant (contributing around 80% of WSIC for all season samples

except for PM₁₀ SUM month) among anions and cations respectively in both fractions (Fig. 6). A decrease in SO₄²⁻ contribution is observed for SUM samples (~47%) in PM₁₀ compared to WIN and POM seasons, however, no significant variation is observed in SO₄²⁻ fraction for PM_{2.5} samples (Fig. 6). Similarly, no significant variation is observed for NH₄⁺ percentage in PM_{2.5}, however a gradual increase in NH₄⁺ contribution to PM₁₀ is observed with lowest during SUM (10%), followed by POM (13%) and highest in WIN (16%). Apart from SO₄²⁻ and NH₄⁺, we observe significant contribution of Ca²⁺, Na⁺, Cl⁻ and NO₃⁻ to PM₁₀, particularly during SUM months, and K⁺ in PM_{2.5} samples. These observations suggest contribution of primary emission (mainly from sea-salt and mineral dust) is significant in PM₁₀, while those from secondary aerosol formation (formed by gas to particle conversion or multiphase chemistry) may be dominant in PM_{2.5}, which is consistent with previous studies from Indian subcontinent (Kumar et al., 2010b; Ram et al., 2012; Rastogi et al., 2015;).

3.3. Chemical species of WSIC and their variation in PM₁₀ and PM_{2.5}:

3.3.1 Sea salt (Na⁺ and Cl⁻):

Sea salts are mainly derived from breaking of sea waves in the marine region (Anguelova and Webster, 2006). By using Na⁺ and Cl⁻ concentration in ambient aerosols, sea-salt concentration can be estimated, presuming that Na⁺ and Cl⁻ ion solely derived from seawater, following this relation (Quinn et al., 2007, Kumar et al., 2008a):

$$\text{Sea Salt} = [\text{Cl}^-] (\mu\text{g m}^{-3}) + 1.47 * [\text{Na}^+] (\mu\text{g m}^{-3})$$

Here, 1.47 is the ratio of (Na⁺+ K⁺+Mg²⁺+ Ca²⁺+SO₄²⁻+HCO₃⁻)/ Na⁺ in seawater (Holland, 1978; Quinn et al., 2004). This approach excludes the contribution of nss-K⁺, Mg²⁺, Ca²⁺, SO₄²⁻, and HCO₃⁻ in the sea-salt mass and allows for the loss of Cl⁻ due to its depletion through chemical reaction. The monthly average trend of sea salt concentration is shown in Fig. 7, as Box-whisker plot and their season average concentration are reported in Table-2a and 2b. A large variation is observed for PM₁₀ samples with higher concentration during SUM season (3.73±1.7 μg m⁻³) compared to WIN (1.89±0.87 μg m⁻³) and POM (1.70±1.29 μg m⁻³) period. On the other hand, no significant variation is found for PM_{2.5} samples except few higher episodic values at the beginning of summer months (Mar-2018 and Feb-2019). These episodic higher values may be attributed to stronger winds from marine region bringing coarse and fine sea-salts to our sampling site, which is also evident from higher sea-salt concentrations in PM₁₀ for Mar-2018 and Feb-2019 (Fig. 7). An increase in sea-salt concentration depends on higher wind speed as well as wind direction and oceanic waves (de Leeuw et al., 2000; Niedermeier et al., 2014). During this study, we have observed relatively higher wind speed during summer months compared to rest of the year. In addition, the winds are mainly derived from marine region during

summer, as evident from the AMBTs (Fig. 2). Thus, the higher values of sea-salt can be attributed to the meteorological condition prevailing at our study site. It is important to mention here, that sea-salts also contribute to other ions (e.g. K^+ , Mg^{2+} , Ca^{2+} and SO_4^{2-}), and thus, sea-salt correction is necessary to assess their temporal variability. The non-sea salt (nss) components have been calculated by using the following equations:

$$nss-X = [X]_{total} - R_{X_{sea-salt}} * [Na^+]_{measured}$$

where, $[X]_{total}$ is measured concentration of specific ion and $R_{X_{sea-salt}}$ is the weight ratio of particular ion to Na^+ in seawater and $[Na^+]_{measured}$ is measured Na^+ concentration in $\mu g m^{-3}$. $R_{X_{sea-salt}}$ for K^+ , Ca^{2+} , Mg^{2+} , and SO_4^{2-} is 0.037, 0.0373, 0.12, and 0.252 respectively (Keene et al., 1986; Sarin et al., 2011; Kumar and Sarin, 2009).

3.3.2 nss- Ca^{2+} and nss- Mg^{2+} :

The presence of nss- Ca^{2+} and nss- Mg^{2+} ion in the ambient aerosol samples typically indicate the contribution of crustal mineral dust (Rastogi and Sarin, 2006; Kumar and Sarin, 2010b). Monthly average concentration and its variation for nss- Ca^{2+} and nss- Mg^{2+} are shown in the box-whisker plot (Fig. 8) and their seasonal average for PM_{10} and $PM_{2.5}$ are reported in Table 2a and 2b. A general increasing trend can be observed in PM_{10} particles for nss- Ca^{2+} concentration (in $\mu g m^{-3}$) while moving from WIN (mean: 0.93 ± 0.64 ; range: 0.36-3.7) to SUM (mean: 1.31 ± 0.72 ; range: 0.36-2.88) season and then it again starts decreasing in POM (mean: 0.67 ± 0.4 ; range: 0.11-0.14) with average comparable value with winter month of 2019. No such significant temporal variability is observed for $PM_{2.5}$. However, relatively lower values (mostly below detection (BD)) were found for nss- Mg^{2+} (Table 2b), with no significant temporal variability as observed for that of nss- Ca^{2+} . Higher concentration of sea-salt corrected calcium during SUM can be attributed to contribution from the arid/semi-arid desert region in the Middle-east (Arabian Peninsula, region bordering Afghanistan-Iran-Pakistan, Sistan basin) as well as Desert region in north-western India (Thar Desert). Air mass back-trajectories are clearly observed to transverse over these regions (Fig. 2) during the SUM months. In contrast, we observe mixed air-masses with dominant contribution from continent (based on cluster analyses; Fig. S3) during POM as well as air-mass from northern/north-eastern India during WIN, can transport mineral dust contributing to nss- Ca^{2+} . In contrast to other locations over India (Kumar and Sarin, 2010b; Ram et al., 2010) we did not observe significant variation in nss- Ca^{2+} during the annual seasonal cycle. For example, over Mt. Abu, a high-altitude site located in western India, increase in summer nss- Ca^{2+} is observed by a factor of two or more than those observed in monsoon and winter season (Kumar and Sarin, 2010b). Similarly, (Ram et al., 2010) have observed an order of magnitude

increase in nss-Ca^{2+} , over Kanpur. However, there are occurrence of dust storms in the Middle-east and Southwest Asia region (Aswini et al., 2020b; Kumar et al., 2020) which can also significantly contribute to nss-Ca^{2+} over our study site. Similar kind of trend for Ca^{2+} was also reported in Agnihotri et. al., (2015) (winter: 2.3 ± 1.4) and in Yadav et. al., (2020) (WM: 1.45 ± 0.57 ; SIM: 2.79 ± 2.22).

3.3.3 Secondary inorganic species (NH_4^+ , NO_3^- , nss-SO_4^{2-}):

Secondary inorganic species are mainly formed via multi-phase chemistry from the precursor gases (ammonia and oxides of sulphur and nitrogen) which are emitted mostly from anthropogenic (fossil fuel and biomass burning) emissions (Seinfeld and Pandis, 2006; Zheng et al., 2020). These secondary species play a vital role in influencing several atmospheric processes acid uptake, enhancing aerosol Fe solubility (Rastogi and Sarin, 2006; Kumar et al. 2010b) impacting on the overall climate in short-term and long-term time scale (Zheng et al., 2020). The monthly distribution of all secondary species is shown as box-whisker plots in Fig. 9 and their seasonal average concentration with minimum and maximum values in PM_{10} and $\text{PM}_{2.5}$ are detailed in Table 2a and 2b respectively. The NH_4^+ and SO_4^{2-} ions were found to co-vary throughout the year with almost similar concentration in PM_{10} and $\text{PM}_{2.5}$. This indicate a significant and dominant contribution of inorganic ions in $\text{PM}_{2.5}$, which is also evident from the plot shown in Fig. S4 and Fig. S5 respectively. Majority of data are falling on or near to 1:1 line, toward $\text{PM}_{2.5}$, which indicate to their dominance in $\text{PM}_{2.5}$. Furthermore, we observed higher values during WIN (PM_{10} NH_4^+ mean: 4.15 ± 1.67 ; range: 0.95-7.48, $\text{PM}_{2.5}$ NH_4^+ mean: 4.37 ± 1.54 ; range: 1.51-8.08 and PM_{10} nss-SO_4^{2-} mean: 14.98 ± 4.74 ; range: 5.06-30.7, $\text{PM}_{2.5}$ nss-SO_4^{2-} mean: 12.72 ± 4.00 ; range: 5.55-25.13) which gradually decreases in SUM (PM_{10} NH_4^+ mean: 2.24 ± 1.33 ; range: 0.29-5.40, $\text{PM}_{2.5}$ NH_4^+ mean: 2.70 ± 1.75 ; range: 0.04-6.77 and PM_{10} nss-SO_4^{2-} mean: 9.30 ± 4.50 ; range: 1.66-19.79, $\text{PM}_{2.5}$ nss-SO_4^{2-} mean: 7.77 ± 4.52 ; range: 0.55-18.20) to lowest value (in May-2018) and start to increase from October-2018 onwards in POM to higher values in WIN-2019. Thus, a clear seasonality can be witnessed from this, however, long-term observation can provide a more robust picture on seasonal variability of these species. Higher concentration of sulphate and nitrate during WIN months can be attributed to local anthropogenic activities as well as winds from north-eastern region of India and/or Indo-Gangetic Plains (IGP), which are relatively more polluted regions, particularly during winter months (Ram et al., 2010). The AMBTs are observed to be derived from the emission regions located in the IGP. However, relatively lower concentration in summer is due to dilution of local anthropogenic emission by relatively pristine air parcel emanating from marine region (Fig. 2), leading to lower concentrations. In post-monsoon season, initially, the concentration is less but gradually increasing in October and November months. This is due to winds which are coming from the southwest during monsoon period were getting reversed to northeast winds as evident from

the air-mass back trajectories shown in Fig. 2. This high contribution of SO_4^{2-} during winters suggest a significant component of secondary inorganic aerosols resulting from emissions of SO_2 by a variety of combustion sources using sulphurous fuels, such as coal and oil which is long range transported by winds from the continental region. However, in summer, although the concentration is very low still most of the winds are coming from marine region which depicts that nss-SO_4^{2-} may be derived from oxidation of DMS (Dimethyl Sulphide).

In contrast to sulphate and ammonium ions, NO_3^- is found almost negligible in $\text{PM}_{2.5}$ as compared to PM_{10} (Fig. 9; Table 2a and 2b; Fig. S6). Moreover, no significant seasonal variability is found for NO_3^- and similar seasonal average observed for WIN (mean: 2.25 ± 1.44 ; range: 0.64-8.67) and SUM (mean: 2.93 ± 1.51 ; range: 0.61-5.60) which are relatively higher than POM (mean: 1.16 ± 0.72 ; range: 0.36-3.5) for PM_{10} samples. NO_3^- is generally formed by the oxidation of NO_x (Wang *et al.*, 2006). This formation of NO_3^- involves the gas-to-particle conversion of NO_x in the ambient atmosphere. Ooki and Uemastu, (2005) reported that nitrate is the dominant constituents associated with the mineral dust rather than the nss-SO_4^{2-} . Relatively higher abundance of nitrate is observed for PM_{10} compared to $\text{PM}_{2.5}$ (shown in box-whisker plot; Fig. 9), during this study and may be attributed to their association with coarser dust as well as sea-salt particle. However, it is not possible to decouple the relative contribution of sea-salt and dust in neutralizing nitrates in the coarse mode using our chemical composition data. Yadav et al (2020), have reported higher abundance of nitrate in PM_{10} and bulk samples, as compared to $\text{PM}_{2.5}$, at coastal site on eastern (Vizag) and western (Goa) North Indian Ocean. Similar enhanced abundance have been found by several studies at high altitude pristine sites (Kumar and Sarin, 2010b) and polluted Indo-Gangetic Plains (Ram et al., 2010).

3.3.4 Biomass burning Species (nss-K^+):

Studies have indicated that concentration of sea-salt corrected potassium (nss-K^+) in fine mode aerosols can serve as a diagnostic tracer for biomass burning source (Andreae, 1983; Andreae and Marlet 2001). However, its contribution from sea-salts and dust sources is highly variable for regional case studies with its dominance in the coarse fraction. Galanter *et al.*, (2000) estimated the geographical distribution of biomass burning to be fairly uniformly distributed over the Indian subcontinent with a maximum in the north-eastern parts. They also estimated that the biomass burning in India takes place mainly during winter and summer (January–May). The monthly average trend for nss-K^+ , in both size fractions, is shown in supplementary material S3. In this study it was found that nss-K^+ ion contribution was found to be maximum during WIN (Fig. S7) i.e. ranged from 0.16 to $2.71 \mu\text{g m}^{-3}$ (Mean: $0.95 \pm 0.38 \mu\text{g m}^{-3}$) and minimum during SUM ranged from BD to $1.28 \mu\text{g m}^{-3}$ (Mean: $0.34 \pm 0.26 \mu\text{g m}^{-3}$) (Fig.S7). During post-monsoon season nss-K^+ ion ranged from BD to 1.47 (Mean:

0.54±0.38 $\mu\text{g m}^{-3}$) in PM_{10} particles. Similarly, in $\text{PM}_{2.5}$ its abundance is maximum in winters i.e. ranged from 0.48 to 2.59 $\mu\text{g m}^{-3}$ (Mean: 1.04±0.31 $\mu\text{g m}^{-3}$) and minimum in summer 0.02 to 1.36 $\mu\text{g m}^{-3}$ (Mean: 0.45±0.35 $\mu\text{g m}^{-3}$). It is important to highlight here that, the relative contribution of nss- K^+ of fine fraction are more than 90 % to total PM_{10} nss- K^+ . This is evident from the $\text{PM}_{2.5}\text{-nss-}\text{K}^+/\text{PM}_{10}\text{-nss}\text{K}^+$ ratio, which found to be 0.94 ± 0.12 , 0.96 ± 0.17 and 0.99 ± 0.03 , during WIN, SUM and POM season. This observation further suggest the dominance of biomass burning tracer in fine fraction as compared to coarser one, particularly during WIN and POM seasons when relatively higher concentrations are found as compared to SUM period. This further points to contribution from long-range transport of aerosols derived from polluted IGP region impacting at coastal region of the Arabian Sea and corroborated by back-trajectories during WIN and POM seasons.

3.4 Major sources of aerosols over Goa

We have observed seasonal variability of various chemical species and their variations have been largely attributed to the distinct wind patterns, primarily discerned by the air-mass back trajectories, during the whole year. In this section, we will further attempt to assess the sources of different chemical species and its relations with meteorology (mainly AMBTs). The $\text{NO}_3^-/\text{nss-SO}_4^{2-}$ ratio typically gives an idea about the contribution from the mobile sources (vehicular emissions) vis-à-vis stationary sources (industrial emissions) (Arimoto et. al., 1996; Kumar and Sarin, 2010b; Yadav et. al., 2020). In this study, the consistently lower ratio (<1) reveals that major contribution of anthropogenic activities is from stationary sources during all the seasons for both the particle classes PM_{10} and $\text{PM}_{2.5}$. It is noteworthy that during WIN in $\text{PM}_{2.5}$, the mean ratio is 0.05 ± 0.04 which is almost 3 times lower than the ratio in PM_{10} 0.17 ± 0.16 . This is due to increase in concentration of nss- SO_4^{2-} in the fine mode aerosol by long-range transport from the Indo-Gangetic Plains (IGP) region which is also supported by our back-trajectory analysis. On the contrary during SUM the mean ratio was 0.61 ± 0.29 for PM_{10} which is almost 7 times higher than that for $\text{PM}_{2.5}$ (0.09 ± 0.10). This is due to increase in NO_3^- concentration in PM_{10} and its uptake by coarser mineral dust and sea-salt particles. An enhanced transport of sea-salt and mineral dust is evident from the increase observed in Na^+ and nss- Ca^{2+} concentration during summer season, which is further supported by the AMBTs (Fig. 2) deriving from Desert and marine regions. These observations are found to similar to those reported by Kumar and Sarin, (2010b) highlighting the role of long range transport of nss- SO_4^{2-} associated with NH_4^+ in fine mode and NO_3^- (associated with crustal species sea-salts). The scatter plot between mass concentrations of nss- SO_4^{2-} and NH_4^+ (Fig. S8) shows a significant correlation for all season, particularly in $\text{PM}_{2.5}$. This clearly suggest the favourable association between secondary sulphate and ammonium ions. We also observed a better correlation between NO_3^- and nss- $\text{Ca}^{2+} + \text{nss-Mg}^{2+} + \text{Na}^+$

(Fig. S9), which establishes association of nitrates with dust and sea-salt, particularly in coarser fraction.

The AMBTs during SUM and POM were mostly derived from Desert region, which are sources of mineral dust, a concomitant increase in nss-Ca^{2+} concentration have been observed during SUM and POM, particularly in PM_{10} fraction. However, no such variability is found for nss-Mg^{2+} . Moreover, very low concentration of nss-Mg^{2+} is found for $\text{PM}_{2.5}$ throughout the year (Table 2b). A scatter plot between nss-Ca^{2+} and nss-Mg^{2+} in PM_{10} (Fig. S10) exhibit relatively poor correlation, highlighting different sources of Ca^{2+} and Mg^{2+} ions. Similar observations were reported by Yadav et al (2020), for aerosols collected at Goa and suggested distinct sources of these ion, which is in contrast to those observed at a semi-arid location in Western India (Kumar and Sarin, 2010b). Such poor correlation can be also attributed to relative contribution of different minerals (calcite vs dolomite) and their chemical processing during long-range transport (Rastogi and Sarin, 2006). Apart for the ions discussed above, the nss-K^+ (typically considered as tracer for biomass burning emissions) concentration is found to be high during end of POM and WIN months (Fig. S7). We noticed a sharp increase in its concentration from September to October and further increase in November. This increase in nss-K^+ is also associated with change in wind trajectories from south westerly to north-easterly as southwest monsoon recedes and northeast Monsoon picks up. During October-November months, crop residue burning is very frequent in the northwestern regions (Punjab, Haryana, and western Uttar Pradesh) of India. The emissions from these sources spread in all directions through long-range transport mechanisms, depending upon the meteorological conditions (Sarkar et al., 2018). Due to change in wind regime, we observe a significant increase in nss-K^+ . This observation further attest to the fact that meteorology play an important role in impacting aerosol concentration and composition at our sampling site.

3.5 Interaction between primary and secondary aerosols in PM_{10} and $\text{PM}_{2.5}$

3.5.1 Chloride deficit:

Sea-salt undergoes heterogeneous phase reaction while interacting with acidic gases and /or secondary aerosols (e.g. HNO_3 and H_2SO_4) causing removal of nascent chlorine via super-saturation of HCl and this is referred as Cl⁻depletion (Sarin et al., 2011). This is significant over the marine or coastal regions due to the impact of polluted air-mass interacting with sea-salts (Struges and Shaw 1993; Johansen et al. 1999; Kumar et al. 2008a, b). Such depletion and emission of reactive chloride (as a free radical) is considered to be an important intermediate in the oxidation reactions associated

with the removal of light hydrocarbons and ozone in the atmosphere (Singh and Kasting 1988; Vogt et al. 1996). Cl^- depletion (%) can be calculated by the following relation (Sarin et al., 2011):

$$\text{Cl}^- \text{ depletion (\%)} = 100[(1.80 \times \text{Na}^+) - \text{Cl}_m] / (1.80 \times \text{Na}^+)$$

Where $1.80 \times \text{Na}^+$ is the Cl^- concentration ($\mu\text{g m}^{-3}$) expected from the sea and Cl_m is the measured Cl^- concentration ($\mu\text{g m}^{-3}$) in the sample. In the present study, we observed lower $\text{Cl}^- / \text{Na}^+$ ratio compared to bulk seawater ratio of 1.80 indicating Cl^- - depletion process, which is observed in all seasons for both PM_{10} and $\text{PM}_{2.5}$. This is also evident from the scatter-plot between mass concentrations (in $\mu\text{g m}^{-3}$) of Na^+ and Cl^- , shown in Fig. 10 for all season. We observe large scatter in data set, showing significant variability in Cl^- depletion process at our study site. Majority of PM_{10} data are falling near to the sea-water line, particularly during SUM season, however, large deviation (from seawater line) is observed for WIN and POM samples. Similar distribution is found for $\text{PM}_{2.5}$ data, although the sea-salt concentration is relatively lower than those observed for PM_{10} (see section 3.3.1). The $\text{Cl}^- / \text{Na}^+$ ratio for PM_{10} was found to be lowest (mean: 0.60 ± 0.30) during WIN as compared to those in POM (mean: 0.75 ± 0.44) and SUM (Mean: 0.82 ± 0.64). However, in $\text{PM}_{2.5}$, we observe lowest ratio in POM (0.41 ± 0.28) compared to almost similar ratio in WIN (1.02 ± 0.48) and SUM (1.09 ± 0.56). This indicates relatively high Cl^- - depletion in PM_{10} (mean = $68.2 \pm 14.3\%$) compared to $\text{PM}_{2.5}$ (mean = $59.1 \pm 21.6\%$) during WIN, almost similar in both fraction (PM_{10} mean = $56.2 \pm 32.4\%$ and $\text{PM}_{2.5}$ mean = $58.4 \pm 22.5\%$) during SUM and high in $\text{PM}_{2.5}$ (mean = $85.8 \pm 10.3\%$) than in PM_{10} (mean = $61.5 \pm 18.8\%$) during POM. This is also evident in Fig. 11, showing average monthly trend of Cl^- depletion. Similar variations (39-78 %) in Cl^- deficit have been reported by (Venkatraman et al., 2002) at an urban site (Mumbai, $19^\circ 23' \text{N}$ and $72^\circ 50' \text{E}$) on west coast of India, in two different sampling periods during January–March. In contrast to such variable Cl^- -deficit, Sarin et al., (2011), have observed very high deficit (ranging from 82 to 98 %) during continental outflow season over the Bay of Bengal. However, large variability (12-100 %) have been reported by (Kumar et al., 2008a) over the Arabian Sea. Such observation clearly demonstrate the role of continental outflow in removing Cl^- from sea-salt which has significant implication towards atmospheric chemistry in the marine atmospheric boundary layer. The released chlorine have potential as an oxidant (Solomon, 1999), which may have role in oxidation of dimethyl sulphide (DMS; Keene et al., 1990) as well as in enhancing tropospheric ozone due to their interaction with volatile organic compounds (Raff et al., 2009) . -In comparison to such high deficit, several studies (Savoie and Prospero 1982; Kerminen et al. 1998; Johansen et al. 1999) have observed relatively lower values (ranging from 20 to 30%) in open oceanic regions, and have attributed to chemical uptake of nss-SO_4^{2-} derived from DMS sources in the open ocean. In this study, we have not

measured the methane sulphonate ions, thus we could not estimate the DMS derived (or biogenic sourced) sulphate.

As discussed previously, acidic species (nitrate and sulphate) play vital role in controlling this process, we will assess their contribution in different size fraction. A scatter plot between equivalent concentrations of ($\text{Cl}^- + \text{NO}_3^-$) and Na^+ is shown in Fig. 12a, to understand the role of nitrate in Cl^- removal following (Sarin et al., 2011). In contrast to the observation of Sarin et al (2011) over the Bay of Bengal, we observed scatter of data on either side of 1:1 line, suggesting the role of both sulphate and nitrate in Cl^- removal process. The concentration of sulphates are 3-10 times higher than nitrates in PM_{10} and order of magnitude higher in $\text{PM}_{2.5}$, which suggest sulphate ions are mostly responsible for Cl^- removal process. However, we noticed majority of PM_{10} samples during all season to fall towards the ($\text{Cl}^- + \text{NO}_3^-$), suggesting contribution from nitrates in controlling this process. The role nitrate in removing sea-salt chloride is well documented in various studies (Wu and Okada, 1994; Quinn and Bates, 2005; Hsu et al., 2007), particularly in coarser fraction compared to fine mode (Pio and Lopes, 1998). In this study, we observed relatively higher ratios of $[\text{Cl}^- + \text{NO}_3^-]$ to Na^+ for WIN (mean: 0.91 ± 0.21) and POM (mean: 0.79 ± 0.24) in PM_{10} as compared to their $\text{PM}_{2.5}$ counterpart (0.79 ± 0.21 and 0.59 ± 0.20 respectively). However, during SUM relatively higher ratio is observed for $\text{PM}_{2.5}$ (mean: 0.94 ± 0.31) than PM_{10} (mean: 0.74 ± 0.30). These observation suggest contribution from nitrate in removing Cl^- from sea-salt, as the overall ratios are higher than those observed for the Bay of Bengal (0.37; Sarin et al., (2011) and the subtropical South China Sea 0.17 (Hsu et al., 2007), where the role of nss-SO_4^{2-} is dominant in controlling this process. We further examined the relationship between NH_4^+ and nss-SO_4^{2-} (in equivalent units; Fig. 12b), where we observed most of the PM_{10} and $\text{PM}_{2.5}$ data are falling on or nearby 1:1 line, indicating a complete neutralization by ammonium ions. The $\text{NH}_4^+/\text{nss-SO}_4^{2-}$ ratio were found to be greater than 1 in $\text{PM}_{2.5}$ during WIN and SUM (1.47 ± 0.14 and 1.06 ± 0.60 respectively) as well as in PM_{10} (1.32 ± 0.23 and 1.09 ± 0.29 respectively). This indicate formation of $(\text{NH}_4)_2\text{SO}_4$ as compared to $(\text{NH}_4)\text{HSO}_4$ in PM_{10} as well as in $\text{PM}_{2.5}$ during WIN and SUM seasons. In contrast, relatively lower ratios were observed for POM (0.81 ± 0.47 for PM_{10} and 0.92 ± 0.31 for $\text{PM}_{2.5}$), which suggest the abundance of $(\text{NH}_4)\text{HSO}_4$ instead of $(\text{NH}_4)_2\text{SO}_4$ or relatively more acidic nature of aerosols controlled by sulphates. We have also observed higher Cl^- deficit during POM compared to SUM and WIN, which can thus be attributed to this excess sulphates over and above that is neutralized by NH_4^+ . Based on cluster analyses (Fig. S3), we have observed AMBTs are mostly derived from the continental sources during POM and the presence of excess nss-SO_4^{2-} can impact on other processes which include chemical processing of iron present in ambient aerosols. This has

significant implication to the supply of labile Fe, which can act as micronutrients, to coastal waters of the Arabian Sea.

3.5.2. Neutralization factor:

Neutralization factor (NF) is an indicator of aerosol acidity and it can be estimated from the ratio of molar concentrations of cations and anions (Wu et. al., 2017; Yadav et. al., 2020). In this study, considering the significant contribution of nss-Ca^{2+} , nss-Mg^{2+} and nss-K^+ , we have used equation for calculation of NF following Yadav et. al., (2020), which is :

$$\text{NF} = ([\text{NH}_4^+] + [\text{Na}^+] + 2*[\text{nss-Ca}^{2+}] + 2*[\text{nss-Mg}^{2+}] + [\text{nss-K}^+]) / (2*[\text{nss-SO}_4^{2-}] + [\text{NO}_3^-] + [\text{Cl}^-])$$

Here, all the ionic concentrations are in $\mu\text{eq m}^{-3}$. A value of $\text{NF} < 1$, indicates acidic nature of ambient aerosol and/or incomplete neutralization, however value of $\text{NF} > 1$ indicates that cations are involved in neutralizing the acidic species of aerosol (Wu et. al., 2017). We observed NF averaging around 1 for $\text{PM}_{2.5}$ (1.00 ± 0.20) except for those collected during POM (0.97 ± 0.11), suggesting a complete neutralization of acidic species in ambient aerosols during WIN and SUM months. Being NH_4^+ , the dominant cation, it plays a key role in neutralizing the acidic species during WIN and SUM in $\text{PM}_{2.5}$. However, either due to lack of ammonium or excess nss-SO_4^{2-} , we observe an incomplete neutralization during POM season. Similarly, near neutrality of ionic species is found for PM_{10} during WIN (0.96 ± 0.07) and SUM (0.97 ± 0.12) months. However, relatively lower NF (0.90 ± 0.07) is shown by POM samples, highlighting the presence of excess acid (more than neutralized by alkaline species). This excess acid can significantly impact on other atmospheric processes including Cl^- -depletion. It is interesting to note here that we have observed relatively higher Cl^- -deficit in PM_{10} and $\text{PM}_{2.5}$ during POM season, which is corroborating our previous interpretation of high Cl^- -deficit (see section 3.5.1). We further compared our results with Yadav et. al., (2020), wherein, they have reported near neutrality for both PM_{10} and $\text{PM}_{2.5}$ and lower NF for TSP suggesting acidic composition at Goa. These results further highlights on increase in neutralization process with decrease in particle grain size (Wu et. al., 2017), which is consistent with our observation as well.

3. Conclusion

We present here, a one-year long aerosol chemical composition data of size-segregated aerosols (PM_{10} and $\text{PM}_{2.5}$) at a costal location in the Northeastern Arabian Sea (Goa; 15.46°N , 73.8°E , 55.8m above the sea level). Following are the major outcome of our study:

1. A uniform dominance of nss-SO_4^{2-} and NH_4^+ is observed in both PM_{10} and $\text{PM}_{2.5}$ in all three seasons, with highest abundance of both species during winter months.

2. A significant temporal variability is observed in sea-salt concentration in PM_{10} with highest values observed during summer; while, no significant temporal variability is found for $PM_{2.5}$ composition.
3. Significant increase in secondary aerosols (SO_4^{2-} and NH_4^+) is observed in $PM_{2.5}$, during winter associated with higher values of nss- K^+ indicating long-range transport of secondary aerosols from the north/northwestern India (IGP). This observation is corroborated with air-mass back trajectory analyses.
4. A remarkable contribution by excess of acidic ions is observed being responsible for significant chloride depletion which is highest during post monsoon months for fine mode aerosols.
5. Neutralization factor is found to be lowest during post monsoon, however, near neutrality is observed for rest of the year.

In addition to confirming the results of previous studies based on shorter measurement periods, this study has regional as well as global importance as it provides quality data set on aerosols water-soluble ionic composition at a regional location in the Northeastern Arabian Sea. Such dataset are helpful in constraining output of the climatic models and give more realistic future projections.

Acknowledgement:

Funding for this research is supported by MoES PMN project. The Department of Science and Technology funded Ashwini Kumar, Govt. of India, under the SPLICE programme. We gratefully acknowledge the NOAA Air Resources Laboratory (ARL) for the provision of the HYSPLIT transport and dispersion model (<http://www.ready.noaa.gov>) used in this publication.

References:

- Agnihotri, R., Karapurkar, S.G., Sarma, V.V.S.S., Yadav, K., Kumar, M.D., Sharma, C., Prasad, M.V.S.N., 2015. Stable isotopic and chemical characteristics of bulk aerosols during winter and summer season at a station in Western Coast of India (Goa). *Aerosol Air Qual. Res.* 15, 888–900. <https://doi.org/10.4209/aaqr.2014.07.0127>.
- Andreae, M. O., (1983), Soot carbon and excess fine potassium: Long-range transport of combustion derived aerosols, *Science*, 220, 1148-1151, 1983
- Andreae, M. O., and Merlet, P. (2001), Emission of trace gases and aerosols from biomass burning, *Global Biogeochem. Cycles*, 15(4), 955– 966, doi:10.1029/2000GB001382.
- Anderson, R.F., 2020. GEOTRACES: Accelerating Research on the Marine Biogeochemical Cycles of Trace Elements and Their Isotopes. *Ann. Rev. Mar. Sci.* 12, 49–85. <https://doi.org/10.1146/annurev-marine-010318-095123>
- Anguelova, M.D., Webster, F., 2006. Whitecap coverage from satellite measurements: A first step toward modeling the variability of oceanic whitecaps. *J. Geophys. Res. Ocean.* 111. <https://doi.org/10.1029/2005JC003158>
- Arimoto, R., Duce, R.A., Savoie, D.L., Prospero, J.M., Talbot, R., Cullen, J.D., Tomza, U., Lewis, N.F., Ray, B.J., 1996. Relationships among aerosol constituents from Asia and North Pacific during PEM-West A. *J. Geophys. Res.* 101, 2011e2023
- Arimoto, R., Duce, R.A., Ray, B.J., Tomza, U., 2003. Dry deposition of trace elements to the western North Atlantic. *Global Biogeochem. Cycles* 17. <https://doi.org/10.1029/2001GB001406>
- Aswini, A.R., Hegde, P., Aryasree, S., Girach, I.A., Nair, P.R., 2020a. Continental outflow of anthropogenic aerosols over Arabian Sea and Indian Ocean during wintertime: ICARB-2018 campaign. *Sci. Total Environ.* 712, 135214. <https://doi.org/10.1016/j.scitotenv.2019.135214>
- Aswini, M.A., Kumar, A., Das, S.K., 2020b. Quantification of long-range transported aeolian dust towards the Indian peninsular region using satellite and ground-based data - A case study during a dust storm over the Arabian Sea. *Atmos. Res.* 239, 104910. <https://doi.org/10.1016/j.atmosres.2020.104910>
- Baker, A.R., Croot, P.L., 2010. Atmospheric and marine controls on aerosol iron solubility in seawater. *Mar. Chem.* 120, 4–13. <https://doi.org/10.1016/j.marchem.2008.09.003>
- Baker, A.R., Adams, C., Bell, T.G., Jickells, T.D., Ganzeveld, L., 2013. Estimation of atmospheric nutrient inputs to the Atlantic Ocean from 50°N to 50°S based on large-scale field sampling: Iron and other dust-associated elements. *Global Biogeochem. Cycles* 27, 755–767. <https://doi.org/10.1002/gbc.20062>
- Baker, A.R., Kanakidou, M., Altieri, K.E., Daskalakis, N., Okin, G.S., Myriokefalitakis, S., Dentener, F., Uematsu, M., Sarin, M.M., Duce, R.A., Galloway, J.N., Keene, W.C., Singh, A., Zamora, L., Lamarque, J.F., Hsu, S.C., Rohekar, S.S., Prospero, J.M., 2017. Observation- and model-based estimates of particulate dry nitrogen deposition to the oceans. *Atmos. Chem. Phys.* 17, 8189–8210. <https://doi.org/10.5194/acp-17-8189-2017>

- Balakrishnan, Kalpana, Santu Ghosh, Gurusamy Thangavel, Sankar Sambandam, Krishnendu Mukhopadhyay, Naveen Puttaswamy, Arulselvan Sadasivam, et al. 2018. “Exposures to Fine Particulate Matter (PM_{2.5}) and Birthweight in a Rural-Urban, Mother-Child Cohort in Tamil Nadu, India.” *Environmental Research* 161 (June 2017): 524–31. <https://doi.org/10.1016/j.envres.2017.11.050>.
- Barnett, T.P., Adam, J.C., Lettenmaier, D.P., 2005. Potential impacts of a warming climate on water availability in snow-dominated regions. *Nature* 438, 303–309. <https://doi.org/10.1038/nature04141>
- Budhavant, K.B., Rao, P.S.P., Safai, P.D., 2017. Size distribution and chemical composition of summer aerosols over Southern Ocean and the Antarctic region. *J. Atmos. Chem.* 74, 491–503. <https://doi.org/10.1007/s10874-016-9356-2>
- Chance, R., Jickells, T.D., Baker, A.R., 2015. Atmospheric trace metal concentrations, solubility and deposition fluxes in remote marine air over the south-east Atlantic. *Mar. Chem.* 177, 45–56. <https://doi.org/10.1016/j.marchem.2015.06.028>
- Chatterjee, A., Adak, A., Singh, A.K., Srivastava, M.K., Ghosh, S.K., Tiwari, S., Devara, P.C.S., Raha, S., 2010. Aerosol chemistry over a high altitude station at northeastern Himalayas, India. *PLoS One* 5. <https://doi.org/10.1371/journal.pone.0011122>
- Cvitešić Kušan, A., Kroflič, A., Grgić, I., Ciglencčki, I., Frka, S., 2020. Chemical characterization of fine aerosols in respect to water-soluble ions at the eastern Middle Adriatic coast. *Environ. Sci. Pollut. Res.* 27, 10249–10264. <https://doi.org/10.1007/s11356-020-07617-7>
- de Leeuw, G., F. P. Neele, M. Hill, M. H. Smith, and E. Vignati (2000), Sea spray aerosol production by waves breaking in the surf zone, *J. Geophys. Res.*, **105**, 29,397– 29,409, doi:[10.1029/2000JD900549](https://doi.org/10.1029/2000JD900549).
- <https://doi.org/10.1126/science.1150369>
- Galanter, M., Levy, H., Carmichael, G.R., 2000. Impacts of biomass burning on tropospheric CO, NO_x, and O₃. *J. Geophys. Res. Atmos.* 105, 6633–6653. <https://doi.org/10.1029/1999JD901113>
- Ganguly, R., Sharma, D., Kumar, P., 2019. Trend analysis of observational PM₁₀ concentrations in Shimla city, India. *Sustain. Cities Soc.* 51, 101719. <https://doi.org/10.1016/j.scs.2019.101719>
- Gautam, A.S., Negi, R.S., Singh, S., Srivastava, A.K., Tiwari, S., Bisht, D.S., 2018. Chemical Characteristics of Atmospheric Aerosol at Alaknanda Valley (Srinagar) in the Central Himalaya Region, India. *Int. J. Environ. Res.* 12, 681–691. <https://doi.org/10.1007/s41742-018-0125-8>
- Gautam, Sneha, Adityaraj Talatiya, Mirang Patel, Karan Chabhadiya, and Pankaj Pathak. 2020. “Personal Exposure to Air Pollutants from Winter Season Bonfires in Rural Areas of Gujarat, India.” *Exposure and Health* 12 (1): 89–97. <https://doi.org/10.1007/s12403-018-0287-9>.
- Govardhan, G., Nanjundiah, R.S., Satheesh, S.K., Krishnamoorthy, K., Kotamarthi, V.R., 2015. Performance of WRF-chem over indian region: Comparison with measurements. *J. Earth Syst. Sci.* 124, 875–896. <https://doi.org/10.1007/s12040-015-0576-7>

- Guieu, C., Al Azhar, M., Aumont, O., Mahowald, N., Levy, M., Ethé, C., Lachkar, Z., 2019. Major Impact of Dust Deposition on the Productivity of the Arabian Sea. *Geophys. Res. Lett.* 46, 6736–6744. <https://doi.org/10.1029/2019GL082770>
- Holland, H. D. (1978), *The Chemistry of the Atmosphere and Oceans*, 154 pp., John Wiley, Hoboken, N. J
- Hsu, S. C., Liu, S. C., Kao, S. J., Jeng, W. L., Huang, Y. T., Tseng, C. M., Tsai, F., Tu, J. Y., and Yang, Y., 2007: Water-soluble species in the marine aerosol from the northern South China Sea: High chloride depletion related to air pollution, *J. Geophys. Res.-Atmos.*, 112, D19304, <https://doi.org/10.1029/2007jd008844>
- Jain, N., Bhatia, A., Pathak, H., 2014. Emission of air pollutants from crop residue burning in India. *Aerosol Air Qual. Res.* 14, 422–430. <https://doi.org/10.4209/aaqr.2013.01.0031>
- Jickells, T.D., An, Z.S., Andersen, K.K., Baker, A.R., Bergametti, G., Brooks, N., Cao, J.J., Boyd, P.W., Duce, R.A., Hunter, K.A., Kawahata, H., Kubilay, N., Laroche, J., Liss, P.S., Mahowald, N., Prospero, J.M., Ridgwell, A.J., Tegen, I., Torres, R., 2005. Global Iron Connections Between Desert Dust, Ocean Biogeochemistry, and Climate. *Science* (80-.). 308, 67–71. <https://doi.org/10.1126/science.1105959>
- Johansen, A.M., Siefert, R.L., Hoffmann, R., et al., 1999. Chemical characterization of ambient aerosol collected during southwest monsoon and intermonsoon season over the Arabian Sea: anions and cations. *Journal of Geophysical Research* 104, 26325–26347. <https://doi.org/10.1029/1999JD900405>
- Johansen, A.M., Hoffmann, M.R., 2003. Chemical characterization of ambient aerosol collected during the northeast monsoon season over the Arabian Sea: Labile-Fe(II) and other trace metals. *J. Geophys. Res. D Atmos.* 108, 1–11. <https://doi.org/10.1029/2002jd003280>
- Jordi, A., Basterretxea, G., Tovar-Sánchez, A., Alastuey, A., Querol, X., 2012. Copper aerosols inhibit phytoplankton growth in the Mediterranean Sea. *Proc. Natl. Acad. Sci. U. S. A.* 109, 21246–21249. <https://doi.org/10.1073/pnas.1207567110>
- Keene, W.C., Pszenny, A.A.P., Galloway, J.N., Hawley, M.E., 1986. Sea-salt corrections and interpretation of constituent ratios in marine precipitation. *J. Geophys. Res.* 91, 6647. <https://doi.org/10.1029/jd091id06p06647>
- Kerminen, V. M., Teinila, K., Hillamo, R., and Pakkanen, T.: Substitution of chloride in sea-salt particles by inorganic and organic anions, *J. Aerosol Sci.*, 29, 929–942, 1998
- Kishore, N., Srivastava, A.K., Nandan, H., Pandey, C.P., Agrawal, S., Singh, N., Soni, V.K., Bisht, D.S., Tiwari, S., Srivastava, M.K., 2019. Long-term (2005–2012) measurements of near-surface air pollutants at an urban location in the Indo-Gangetic Basin. *J. Earth Syst. Sci.* 128, 1–13. <https://doi.org/10.1007/s12040-019-1070-4>
- Kulshrestha, U.C., Saxena, A., Kumar, N., Kumari, K.M., Srivastava, S.S., 1998. Chemical composition and association of size-differentiated aerosols at a suburban site in a semi-arid tract of India. *J. Atmos. Chem.* 29, 109–118. <https://doi.org/10.1023/A:1005796400044>

- Kumar, A., Sarin, M.M., Sudheer, A.K., 2008a. Mineral and anthropogenic aerosols in Arabian Sea-atmospheric boundary layer: Sources and spatial variability. *Atmos. Environ.* 42, 5169–5181. <https://doi.org/10.1016/j.atmosenv.2008.03.004>
- Kumar, A., Sudheer, A.K., Sarin, M.M., 2008b. Chemical characteristics of aerosols in MABL of bay of Bengal and Arabian sea during spring inter-monsoon: A comparative study. *J. Earth Syst. Sci.* 117, 325–332. <https://doi.org/10.1007/s12040-008-0035-9>
- Kumar, A., Sarin, M.M., 2009 Mineral aerosols from western India: Temporal variability of coarse and fine atmospheric dust and elemental characteristics. *Atmos. Environ.* 43, 4005–4013. <https://doi.org/10.1016/j.atmosenv.2009.05.014>
- Kumar, A., Sarin, M.M., 2010a. Aerosol iron solubility in a semi-arid region: Temporal trend and impact of anthropogenic sources. *Tellus, Ser. B Chem. Phys. Meteorol.* 62, 125–132. <https://doi.org/10.1111/j.1600-0889.2009.00448.x>
- Kumar, A., Sarin, M.M., 2010b. Atmospheric water-soluble constituents in fine and coarse mode aerosols from high-altitude site in western India: Long-range transport and seasonal variability. *Atmos. Environ.* 44, 1245–1254. <https://doi.org/10.1016/j.atmosenv.2009.12.035>
- Kumar, A., Sarin, M.M., Srinivas, B., 2010. Aerosol iron solubility over Bay of Bengal: Role of anthropogenic sources and chemical processing. *Mar. Chem.* 121, 167–175. <https://doi.org/10.1016/j.marchem.2010.04.005>
- Kumar, A., Suresh, K., Rahaman, W., 2020. Geochemical characterization of modern aeolian dust over the Northeastern Arabian Sea: Implication for dust transport in the Arabian Sea. *Sci. Total Environ.* 729, 138576. <https://doi.org/10.1016/j.scitotenv.2020.138576>
- Lawrence, Alfred J., and Ajay Taneja. 2005. “An Investigation of Indoor Air Quality in Rural Residential Houses in India - A Case Study.” *Indoor and Built Environment* 14 (3–4): 321–29. <https://doi.org/10.1177/1420326X05054323>.
- Madhavan, B.L., Niranjana, K., Sreekanth, V., Sarin, M.M., Sudheer, A.K., 2008. Aerosol characterization during the summer monsoon period over a tropical coastal Indian station, Visakhapatnam. *J. Geophys. Res. Atmos.* 113. <https://doi.org/10.1029/2008JD010272>
- Mahowald, N.M., Baker, A.R., Bergametti, G., Brooks, N., Duce, R.A., Jickells, T.D., Kubilay, N., Prospero, J.M., Tegen, I., 2005. Atmospheric global dust cycle and iron inputs to the ocean. *Global Biogeochem. Cycles* 19. <https://doi.org/10.1029/2004GB002402>
- Mehra, P., Prabhudesai, R.G., Joseph, A., Vijay, K., Dabholkar, N., Prabhudesai, S., Nagvekar, S. and Agarvadekar, Y. (2005). Endurance and Stability of Some Surface Meteorological Sensors under Land- and Ship-Based Operating Environments. *Proceedings of the National Symposium on Ocean Electronics, SYMPOL- 2005*, 15–16 December 2005, p. 257–264.
- Mehta, M., Singh, R., Singh, A., Singh, N., Anshumali, 2016. Recent global aerosol optical depth variations and trends - A comparative study using MODIS and MISR level 3 datasets. *Remote Sens. Environ.* 181, 137–150. <https://doi.org/10.1016/j.rse.2016.04.004>

- Michael, M., Yadav, A., Tripathi, S.N., Kanawade, V.P., Gaur, A., Sadavarte, P., Venkataraman, C., 2013. Simulation of trace gases and aerosols over the Indian domain: evaluation of the WRF-Chem Model. *Atmos. Chem. Phys. Discuss.* 13, 12287–12336. <https://doi.org/10.5194/acpd-13-12287-2013>
- Michael, M., Yadav, A., Tripathi, S.N., Kanawade, V.P., Gaur, A., Sadavarte, P., Venkataraman, C., 2014. Simulation of trace gases and aerosols over the Indian domain: evaluation of the WRF-Chem model. *Geosci. Model Dev. Discuss.* 7, 431–482. <https://doi.org/10.5194/gmdd-7-431-2014>
- Momin, G.A., Rao, P.S.P., Safai, P.D., Ali, K., Naik, M.S., Pillai, A.G., 1999. Atmospheric aerosol characteristic studies at Pune and Thiruvananthapuram during INDOEX programme - 1998. *Curr. Sci.*
- Moorthy, K.K., Beegum, S.N., Srivastava, N., Satheesh, S.K., Chin, M., Blond, N., Babu, S.S., Singh, S., 2013. Performance evaluation of chemistry transport models over India. *Atmos. Environ.* 71, 210–225. <https://doi.org/10.1016/j.atmosenv.2013.01.056>
- Mukherjee, S., Singla, V., Pandithurai, G., Safai, P.D., Meena, G.S., Dani, K.K., Anil Kumar, V., 2018. Seasonal variability in chemical composition and source apportionment of sub-micron aerosol over a high altitude site in Western Ghats, India. *Atmos. Environ.* 180, 79–92. <https://doi.org/10.1016/j.atmosenv.2018.02.048>
- Niedermeier, N., Held, A., Müller, T., Heinold, B., Schepanski, K., Tegen, I., Kandler, K., Ebert, M., Weinbruch, S., Read, K., Lee, J., Fomba, K. W., Müller, K., Herrmann, H., and Wiedensohler, A.: Mass deposition fluxes of Saharan mineral dust to the tropical northeast Atlantic Ocean: an intercomparison of methods, *Atmos. Chem. Phys.*, 14, 2245–2266,. <https://doi:10.5194/acp-14-2245-2014>, 2014
- Ng, N.L., Herndon, S.C., Trimborn, A., Canagaratna, M.R., Croteau, P.L., Onasch, T.B., Sueper, D., Worsnop, D.R., Zhang, Q., Sun, Y.L., Jayne, J.T., 2011. An Aerosol Chemical Speciation Monitor (ACSM) for routine monitoring of the composition and mass concentrations of ambient aerosol. *Aerosol Sci. Technol.* 45, 780–794. <https://doi.org/10.1080/02786826.2011.560211>
- Ningombam, S.S., Dumka, U.C., Srivastava, A.K., Song, H.J., 2020. Optical and physical properties of aerosols during active fire events occurring in the Indo-Gangetic Plains: Implications for aerosol radiative forcing. *Atmos. Environ.* 223, 117225. <https://doi.org/10.1016/j.atmosenv.2019.117225>
- Ojha, Narendra, Amit Sharma, Manish Kumar, Imran Girach, Tabish U. Ansari, Som K. Sharma, Narendra Singh, Andrea Pozzer, and Sachin S. Gunthe. 2020. “On the Widespread Enhancement in Fine Particulate Matter across the Indo-Gangetic Plain towards Winter.” *Scientific Reports* 10 (1): 1–9. <https://doi.org/10.1038/s41598-020-62710-8>.
- Ooki, A., Uematsu, M., 2005. Chemical interactions between mineral dust particles and acid gases during Asian dust events. *J. Geophys. Res. D Atmos.* 110, 1–13. <https://doi.org/10.1029/2004JD004737>
- Pan, X., Uno, I., Wang, Zhe, Yamamoto, S., Hara, Y., Wang, Zifa, 2018. Seasonal variabilities in chemical compounds and acidity of aerosol particles at urban site in the west Pacific. *Environ. Pollut.* 237, 868–877. <https://doi.org/10.1016/j.envpol.2017.11.089>

- Pant, P., Harrison, R.M., 2012. Critical review of receptor modelling for particulate matter: A case study of India. *Atmos. Environ.* 49, 1–12. <https://doi.org/10.1016/j.atmosenv.2011.11.060>
- Paytan, A., R.M.Mackeya, K., Chena, Y., Lima, I.D., Doney, S.C., Mahowald, N., Labiosa, R., Post, A.F., 2009. Toxicity of atmospheric aerosols on marine phytoplankton. *PNAS* 106, 4601–4605. <https://doi.org/www.pnas.org/cgi/doi/10.1073/pnas.0811486106>
- Petit, J.E., Favez, O., Sciare, J., Crenn, V., Sarda-Estève, R., Bonnaire, N., Močnik, G., Dupont, J.C., Haeffelin, M., Leoz-Garziandia, E., 2015. Two years of near real-time chemical composition of submicron aerosols in the region of Paris using an Aerosol Chemical Speciation Monitor (ACSM) and a multi-wavelength Aethalometer. *Atmos. Chem. Phys.* 15, 2985–3005. <https://doi.org/10.5194/acp-15-2985-2015>.
- Pio, C. A., & Lopes, D. A. (1998). Chlorine loss from marine aerosol in a coastal atmosphere. *Journal of Geophysical Research: Atmospheres*, 103(D19), 25263-25272.
- Pöschl, U., 2005. Atmospheric aerosols: Composition, transformation, climate and health effects. *Angew. Chemie - Int. Ed.* 44, 7520–7540. <https://doi.org/10.1002/anie.200501122>
- Powell, C.F., Baker, A.R., Jickells, T.D., W. Bange, H., Chance, R.J., Yodle, C., 2015. Estimation of the atmospheric flux of nutrients and trace metals to the eastern tropical North Atlantic Ocean. *J. Atmos. Sci.* 72, 4029–4045. <https://doi.org/10.1175/JAS-D-15-0011.1>
- Raff, J.D., et al. 2009. Chlorine activation indoors and outdoors via surface mediated reactions of nitrogen oxides with hydrogen chloride. *Proc Natl Acad Sci* 106, 13647–13654
- Savoie, D.L., Prospero, J.M.: (1982). Particle size distribution of nitrate and sulfate in the marine atmosphere. *Geophys Res Lett* 9, 1207–1210.
- Solomon, S., 1999. Stratospheric ozone depletion: A review of concepts and history. *Rev Geophys* 37, 275–316
- Quinn, P.K., Coffman, D.J., Bates, T.S., Welton, E.J., Covert, D.S., Miller, T.L., Johnson, J.E., Maria, S., Russell, L., Arimoto, R., Carrico, C.M., Rood, M.J., Anderson, J., 2004. Aerosol optical properties measured on board the Ronald H. Brown during ACE-Asia as a function of aerosol chemical composition and source region. *J. Geophys. Res. D Atmos.* 109, 1–28. <https://doi.org/10.1029/2003JD004010>
- Quinn, P. K. and Bates, T. S., 2005. Regional aerosol properties: Comparisons of boundary layer measurements from ACE 1, ACE 2, aerosols99, INDOEX, ACE asia, TARFOX, and NEAQS, *J. Geophys. Res.-Atmos.*, 110, D14202. <https://doi:10.1029/2004JD004755>
- Quinn, P.K., Shaw, G., Andrews, E., Dutton, E.G., Ruoho-Airola, T., Gong, S.L., 2007. Arctic haze: Current trends and knowledge gaps. *Tellus, Ser. B Chem. Phys. Meteorol.* 59, 99–114. <https://doi.org/10.1111/j.1600-0889.2006.00236.x>
- Ram, K., Sarin, M.M., Tripathi, S.N., 2010. A 1 year record of carbonaceous aerosols from an urban site in the Indo-Gangetic Plain: Characterization, sources, and temporal variability. *J. Geophys. Res. Atmos.* 115. <https://doi.org/10.1029/2010JD014188>

- Ram, K., Sarin, M.M., Sudheer, A.K., Rengarajan, R., 2012. Carbonaceous and secondary inorganic aerosols during wintertime fog and haze over urban sites in the Indo-Gangetic plain. *Aerosol Air Qual. Res.* 12, 355–366. <https://doi.org/10.4209/aaqr.2011.07.0105>
- Ramanathan, V., Crutzen, P.J., Kiehl, J.T., Rosenfeld, D., 2001. Aerosols, Climate, and the Hydrological Cycle. *Science* (80-.). 294, 2119–2124. <https://doi.org/DOI:10.1126/science.1064034>
- Rana, A., Jia, S., Sarkar, S., 2019. Black carbon aerosol in India: A comprehensive review of current status and future prospects. *Atmos. Res.* 218, 207–230. <https://doi.org/10.1016/j.atmosres.2018.12.002>
- Rastogi, N., Sarin, M.M., 2005. Long-term characterization of ionic species in aerosols from urban and high-altitude sites in western India: Role of mineral dust and anthropogenic sources. *Atmos. Environ.* 39, 5541–5554. <https://doi.org/10.1016/j.atmosenv.2005.06.011>
- Rastogi, N., Sarin, M.M., 2006. Chemistry of aerosols over a semi-arid region: Evidence for acid neutralization by mineral dust. *Geophys. Res. Lett.* 33, 10–13. <https://doi.org/10.1029/2006GL027708>
- Rastogi, N., Patel, A., Singh, A., Singh, D., 2015. Diurnal variability in secondary organic aerosol formation over the indo-gangetic plain during winter using online measurement of water-soluble organic carbon. *Aerosol Air Qual. Res.* 15, 2225–2231. <https://doi.org/10.4209/aaqr.2015.02.0097>
- Rastogi, N., Agnihotri, R., Sawlani, R., Patel, A., Babu, S.S., Satish, R., 2020. Chemical and isotopic characteristics of PM10 over the Bay of Bengal: Effects of continental outflow on a marine environment. *Sci. Total Environ.* 726, 138438. <https://doi.org/10.1016/j.scitotenv.2020.138438>
- Sahai, S., Sharma, C., Singh, S.K., Gupta, P.K., 2011. Assessment of trace gases, carbon and nitrogen emissions from field burning of agricultural residues in India. *Nutr. Cycl. Agroecosystems* 89, 143–157. <https://doi.org/10.1007/s10705-010-9384-2>
- Sarin, M., Kumar, A., Srinivas, B., Sudheer, A.K., Rastogi, N., 2011. Anthropogenic sulphate aerosols and large Cl-deficit in marine atmospheric boundary layer of tropical Bay of Bengal. *J. Atmos. Chem.* 66, 1–10. <https://doi.org/10.1007/s10874-011-9188-z>
- Sarkar, S., Singh, R. P., & Chauhan, A. (2018). Crop residue burning in northern India: Increasing threat to Greater India. *Journal of Geophysical Research: Atmospheres*, 123, 6920–6934. <https://doi.org/10.1029/2018JD028428>
- Saxena, M., Sharma, S.K., Tomar, N., Ghayas, H., Sen, A., Garhwal, R.S., Gupta, N.C., Mandal, T.K., 2016. Residential biomass burning emissions over Northwestern Himalayan region of India: Chemical characterization and budget estimation. *Aerosol Air Qual. Res.* 16, 504–518. <https://doi.org/10.4209/aaqr.2015.04.0237>
- Sen, A., Abdelmaksoud, A.S., Nazeer Ahammed, Y., Alghamdi, M.◌., Banerjee, T., Bhat, M.A., Chatterjee, A., Choudhuri, A.K., Das, T., Dhir, A., Dhyani, P.P., Gadi, R., Ghosh, S., Kumar, K., Khan, A.H., Khoder, M., Maharaj Kumari, K., Kuniyal, J.C., Kumar, M., Lakhani, A., Mahapatra, P.S., Naja, M., Pal, D., Pal, S., Rafiq, M., Romshoo, S.A., Rashid, I., Saikia, P., Shenoy, D.M., Sridhar, V., Verma, N., Vyas, B.M., Saxena, M., Sharma, A., Sharma, S.K., Mandal, T.K., 2017. Variations in particulate matter over Indo-Gangetic Plains and Indo-

- Himalayan Range during four field campaigns in winter monsoon and summer monsoon: Role of pollution pathways. *Atmos. Environ.* 154, 200–224. <https://doi.org/10.1016/j.atmosenv.2016.12.054>
- Seinfeld, J. H. & Pandis, S. N. *Atmospheric Chemistry and Physics: From Air Pollution to Climate Change*. Hoboken, NJ: John Wiley and Sons, Inc., 2006.
- Sharma, S.K., Sharma, A., Saxena, M., Choudhary, N., Masiwal, R., Mandal, T.K., Sharma, C., 2016. Chemical characterization and source apportionment of aerosol at an urban area of Central Delhi, India. *Atmos. Pollut. Res.* 7, 110–121. <https://doi.org/10.1016/j.apr.2015.08.002>
- Shrestha, A.B., Wake, C.P., Dibb, J.E., 1997. Chemical composition of aerosol and snow in the high Himalaya during the summer monsoon season. *Atmos. Environ.* 31, 2815–2826. [https://doi.org/10.1016/S1352-2310\(97\)00047-2](https://doi.org/10.1016/S1352-2310(97)00047-2)
- Siefert, R.L., Johansen, A.M., Hoffmann, M.R., 1999. Chemical characterization of ambient aerosol collected during the southwest monsoon and intermonsoon seasons over the Arabian Sea: Labile-Fe(II) and other trace metals. *J. Geophys. Res. Atmos.* 104, 3511–3526. <https://doi.org/10.1029/1998JD100067>
- Singh, H.B., Kasting, J.F.: Chlorine-hydrocarbon photochemistry in the marine troposphere and lower stratosphere. *J Atmos Chem* 7, 261–285 (1988)
- Srinivas, B., Sarin, M.M., 2013a. Atmospheric dry-deposition of mineral dust and anthropogenic trace metals to the Bay of Bengal. *J. Mar. Syst.* 126, 56–68. <https://doi.org/10.1016/j.jmarsys.2012.11.004>
- Srinivas, B., Sarin, M.M., 2013b. Atmospheric deposition of N, P and Fe to the Northern Indian Ocean: Implications to C- and N-fixation. *Sci. Total Environ.* 456–457, 104–114. <https://doi.org/10.1016/j.scitotenv.2013.03.068>
- Srinivas, B., Haque, M.M., Sarin, M., Kawamura, K., 2019. Tracing the Relative Significance of Primary versus Secondary Organic Aerosols from Biomass Burning Plumes over Coastal Ocean Using Sugar Compounds and Stable Carbon Isotopes. *ACS Earth Sp. Chem.* 3, 1471–1484. <https://doi.org/10.1021/acsearthspacechem.9b00140>
- Srivastava, A.K., Singh, S., Tiwari, S., Bisht, D.S., 2012. Contribution of anthropogenic aerosols in direct radiative forcing and atmospheric heating rate over Delhi in the Indo-Gangetic Basin. *Environ. Sci. Pollut. Res.* 19, 1144–1158. <https://doi.org/10.1007/s11356-011-0633-y>
- Streets, D.G., Bond, T.C., Carmichael, G.R., Fernandes, S.D., Fu, Q., He, D., Klimont, Z., Nelson, S.M., Tsai, N.Y., Wang, M.Q., Woo, J.H., Yarber, K.F., 2003. An inventory of gaseous and primary aerosol emissions in Asia in the year 2000. *J. Geophys. Res. Atmos.* 108. <https://doi.org/10.1029/2002jd003093>
- Sturges, W.T., Shaw, G.E., 1993. Halogens in aerosol in central Alaska, *Atmos. Environ.*, 27, 2969–2977
- Sullivan, R.C., Guazzotti, S.A., Sodeman, D.A., Prather, K.A., 2007. Direct observations of the atmospheric processing of Asian mineral dust. *Atmos. Chem. Phys.* 7, 1213–1236. <https://doi.org/10.5194/acp-7-1213-2007>

- Sun, Y., Wang, Z., Dong, H., Yang, T., Li, J., Pan, X., Chen, P., Jayne, J.T., 2012. Characterization of summer organic and inorganic aerosols in Beijing, China with an Aerosol Chemical Speciation Monitor. *Atmos. Environ.* 51, 250–259. <https://doi.org/10.1016/j.atmosenv.2012.01.013>
- Stein, A.F., Draxler, R.R., Rolph, G.D., Stunder, B.J.B., Cohen, M.D., and Ngan, F., (2015). NOAA's HYSPLIT atmospheric transport and dispersion modeling system, *Bull. Amer. Meteor. Soc.*, 96, 2059-2077, <http://dx.doi.org/10.1175/BAMS-D-14-00110.1>
- Sturges, W.T., Shaw, G.E.: Halogens in aerosol in central Alaska, *Atmos. Environ.*, 27, 2969–2977 (1993)
- Tare, V., Tripathi, S.N., Chinnam, N., Srivastava, A.K., Dey, S., Manar, M., Kanawade, V.P., Agarwal, A., Kishore, S., Lal, R.B., Sharma, M., 2006. Measurements of atmospheric parameters during Indian Space Research Organization Geosphere Biosphere Program Land Campaign II at a typical location in the Ganga basin: 2. Chemical properties. *J. Geophys. Res. Atmos.* 111. <https://doi.org/10.1029/2006JD007279>
- Thomas, A., Sarangi, C., Kanawade, V.P., 2019. Recent Increase in Winter Hazy Days over Central India and the Arabian Sea. *Sci. Rep.* 9, 1–10. <https://doi.org/10.1038/s41598-019-53630-3>
- Tiwari, S., Bisht, D.S., Srivastava, A.K., Pipal, A.S., Taneja, A., Srivastava, M.K., Attri, S.D., 2014. Variability in atmospheric particulates and meteorological effects on their mass concentrations over Delhi, India. *Atmos. Res.* 145–146, 45–56. <https://doi.org/10.1016/j.atmosres.2014.03.027>
- van Pinxteren, M., Fiedler, B., van Pinxteren, D., Iinuma, Y., Körtzinger, A., Herrmann, H., 2015. Chemical characterization of sub-micrometer aerosol particles in the tropical Atlantic Ocean: marine and biomass burning influences. *J. Atmos. Chem.* 72, 105–125. <https://doi.org/10.1007/s10874-015-9307-3>
- Venkataraman, C., Reddy, C.K., Josson, S., Reddy, M.S., 2002. Aerosol size and chemical characteristics at Mumbai, India, during the INDOEX-IFP (1999). *Atmos. Environ.* 36, 1979–1991. [https://doi.org/10.1016/S1352-2310\(02\)00167-X](https://doi.org/10.1016/S1352-2310(02)00167-X)
- Venkataraman, C., Habib, G., Kadamba, D., Shrivastava, M., Leon, J.F., Crouzille, B., Boucher, O., Streets, D.G., 2006. Emissions from open biomass burning in India: Integrating the inventory approach with high-resolution Moderate Resolution Imaging Spectroradiometer (MODIS) active-fire and land cover data. *Global Biogeochem. Cycles* 20, 1–12. <https://doi.org/10.1029/2005GB002547>
- Measures, C. I., & Vink, S. (1999). Seasonal variations in the distribution of Fe and Al in the surface waters of the Arabian Sea. *Deep Sea Research Part II: Topical Studies in Oceanography*, 46(8-9), 1597-1622.
- Vogt, R., P. J. Crutzen, R. Sander, A mechanism for halogen release in the remote marine boundary layer, *Nature*, **383**, 327–330, 1996.
- Wang, H., Shooter, D., 2001. Water soluble ions of atmospheric aerosols in three New Zealand cities: Seasonal changes and sources. *Atmos. Environ.* 35, 6031–6040. [https://doi.org/10.1016/S1352-2310\(01\)00437-X](https://doi.org/10.1016/S1352-2310(01)00437-X)

- Wang, W., Liu, H., Yue, X., Li, H., Chen, J., Ren, L., Tang, D., Hatakeyama, S., Takami, A., 2006. Study on acidity and acidic buffering capacity of particulate matter over Chinese eastern coastal areas in spring. *J. Geophys. Res. Atmos.* 111, 1–11. <https://doi.org/10.1029/2005JD006753>
- Williams, B.J., Goldstein, A.H., Millet, D.B., Holzinger, R., Kreisberg, N.M., Hering, S. V., White, A.B., Worsnop, D.R., Allan, J.D., Jimenez, J.L., 2007. Chemical speciation of organic aerosol during the International Consortium for Atmospheric Research on Transport and Transformation 2004: Results from in situ measurements. *J. Geophys. Res. Atmos.* 112, 1–14. <https://doi.org/10.1029/2006JD007601>
- Woo, J.H., Streets, D.G., Carmichael, G.R., Tang, Y., Yoo, B., Lee, W.C., Thongboonchoo, N., Pinnock, S., Kurata, G., Uno, I., Fu, Q., Vay, S., Sachse, G.W., Blake, D.R., Fried, A., Thornton, D.C., 2003. Contribution of biomass and biofuel emissions to trace gas distributions in Asia during the TRACE-P experiment. *J. Geophys. Res. Atmos.* 108. <https://doi.org/10.1029/2002jd003200>
- Wu, P.M., Okada, K.: Nature of coarse nitrate particles in the atmosphere – a single particle approach, *Atmos. Environ.*, 28, 2053–2060 (1994)
- Wu, X., Deng, J., Chen, J., Hong, Y., Xu, L., Yin, L., ... & Yuan, C. S. (2017). Characteristics of water-soluble inorganic components and acidity of PM_{2.5} in a coastal city of China. *Aerosol and Air Quality Research*, 17(9), 2152-2164.
- Yadav, K., Sarma, V.V.S.S., Kumar, M.D., 2020. Spatial and temporal variability in concentration and characteristics of aerosols at Visakhapatnam (east) and Goa (west) coasts of India. *Environ. Sci. Pollut. Res.* 27, 532–546. <https://doi.org/10.1007/s11356-019-06784-6>
- Zheng, Guangjie, Hang Su, Siwen Wang, Meinrat O. Andreae, Ulrich Pöschl, and Yafang Cheng. 2020. “Multiphase Buffer Theory Explains Contrasts in Atmospheric Aerosol Acidity.” *Science (New York, N.Y.)* 369 (6509): 1374–77. <https://doi.org/10.1126/science.aba3719>.

Figures:

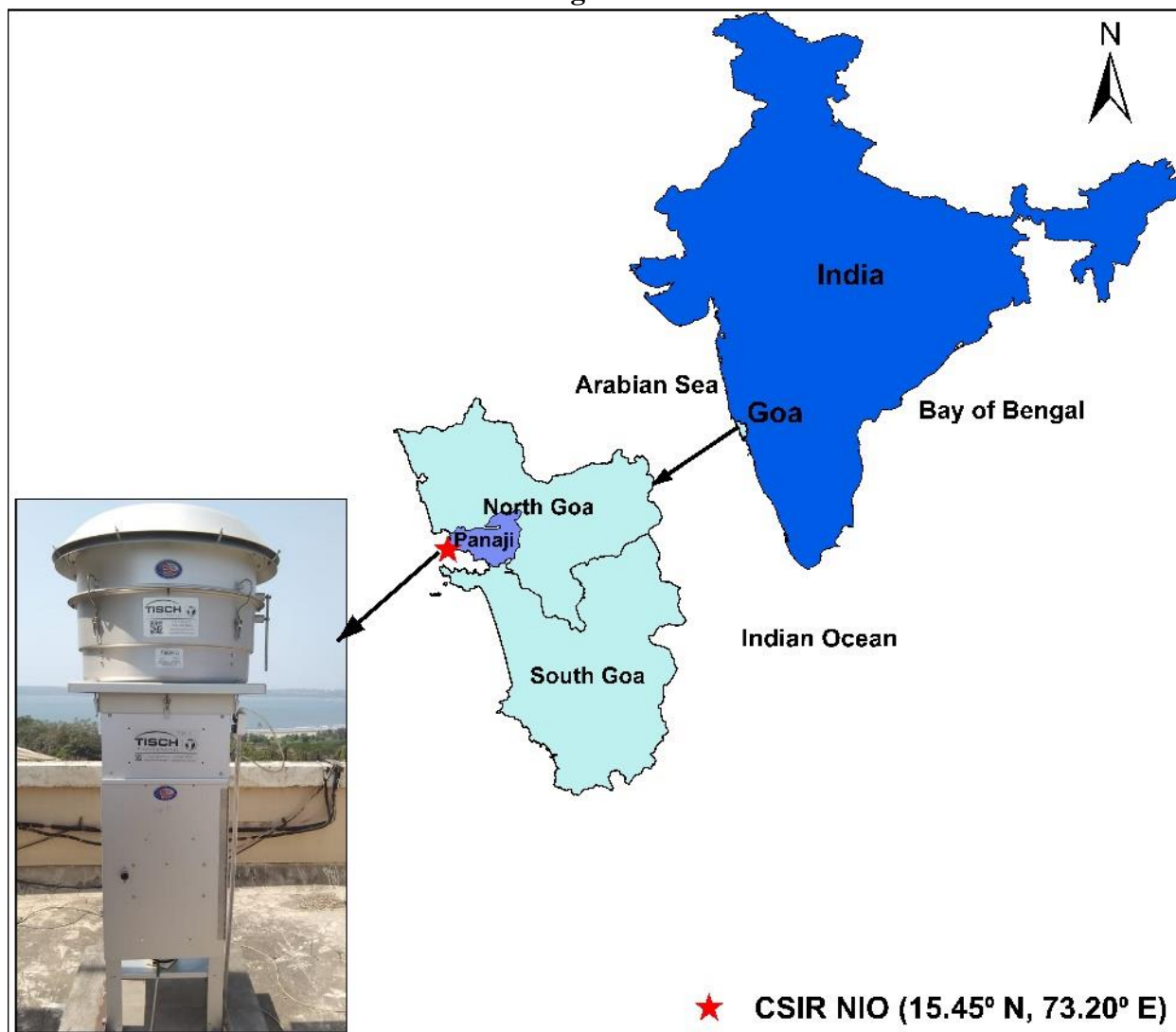


Fig .1: Location of bulk aerosol sampling at the roof of National Institute of Oceanography Goa (at a height 56 meter above sea level; 15.45°N, 73.20°E).

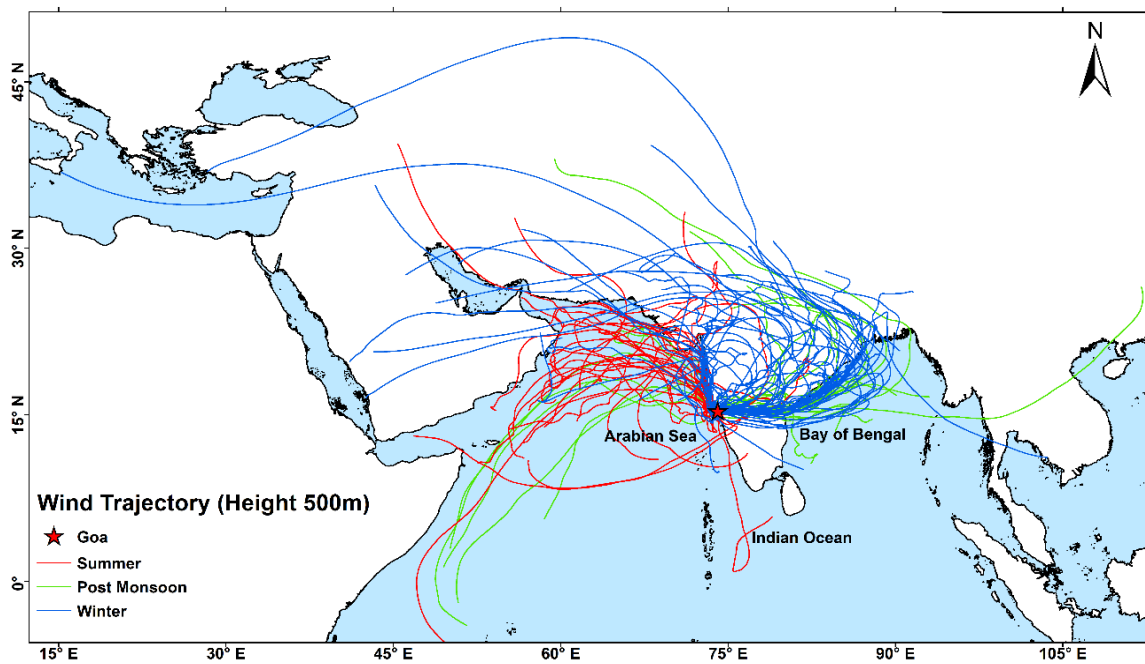


Fig. 2: 7-days back trajectories at 500 m for sampling days ending at our sampling site. AMBTs were computed using HYSPLIT-4 model and GDAS dataset of National Oceanic and Atmospheric Administration Air Resource Laboratory (NOAA) at 500 m altitude (Stein et al., 2015) for this study.

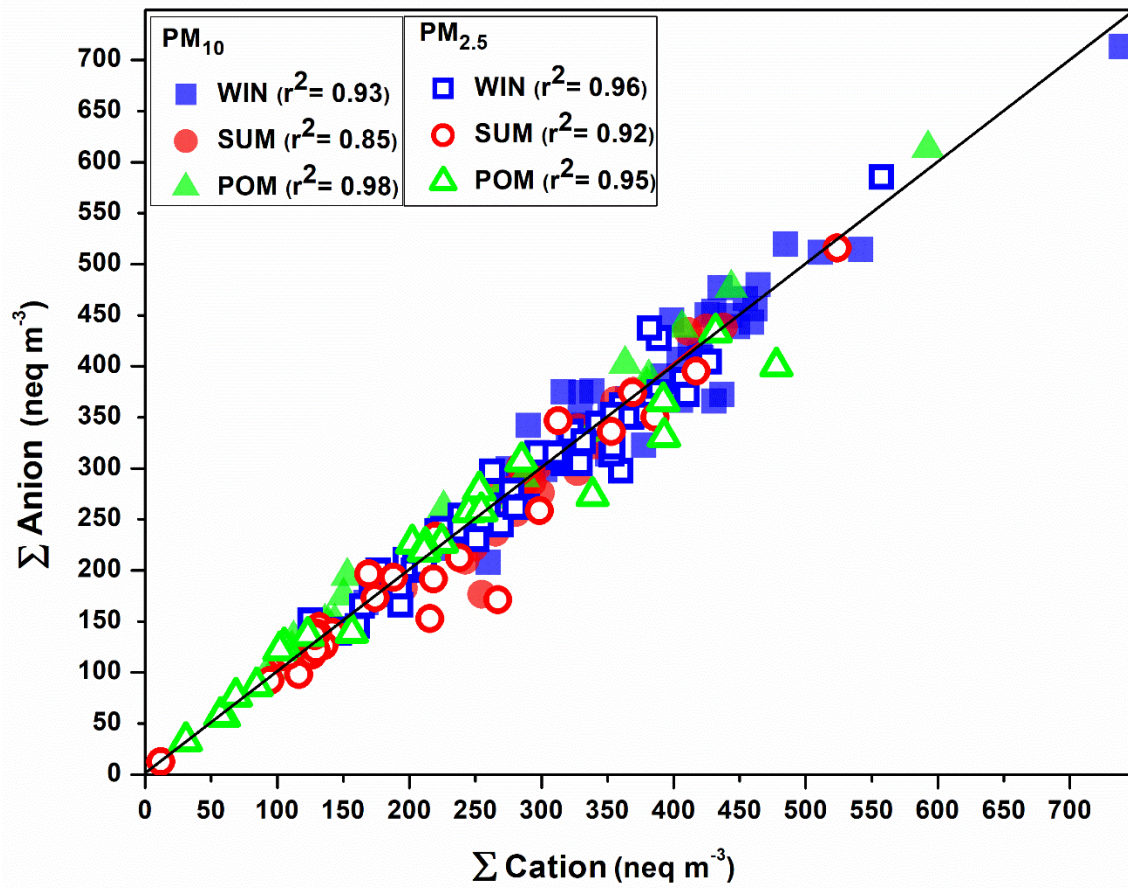


Fig. 3. Seasonal correlation plot between total cation (sum of Na^+ , NH_4^+ , K^+ , Mg^{2+} , Ca^{2+}) and total anion (sum of Cl^- , NO_3^- , SO_4^{2-}).

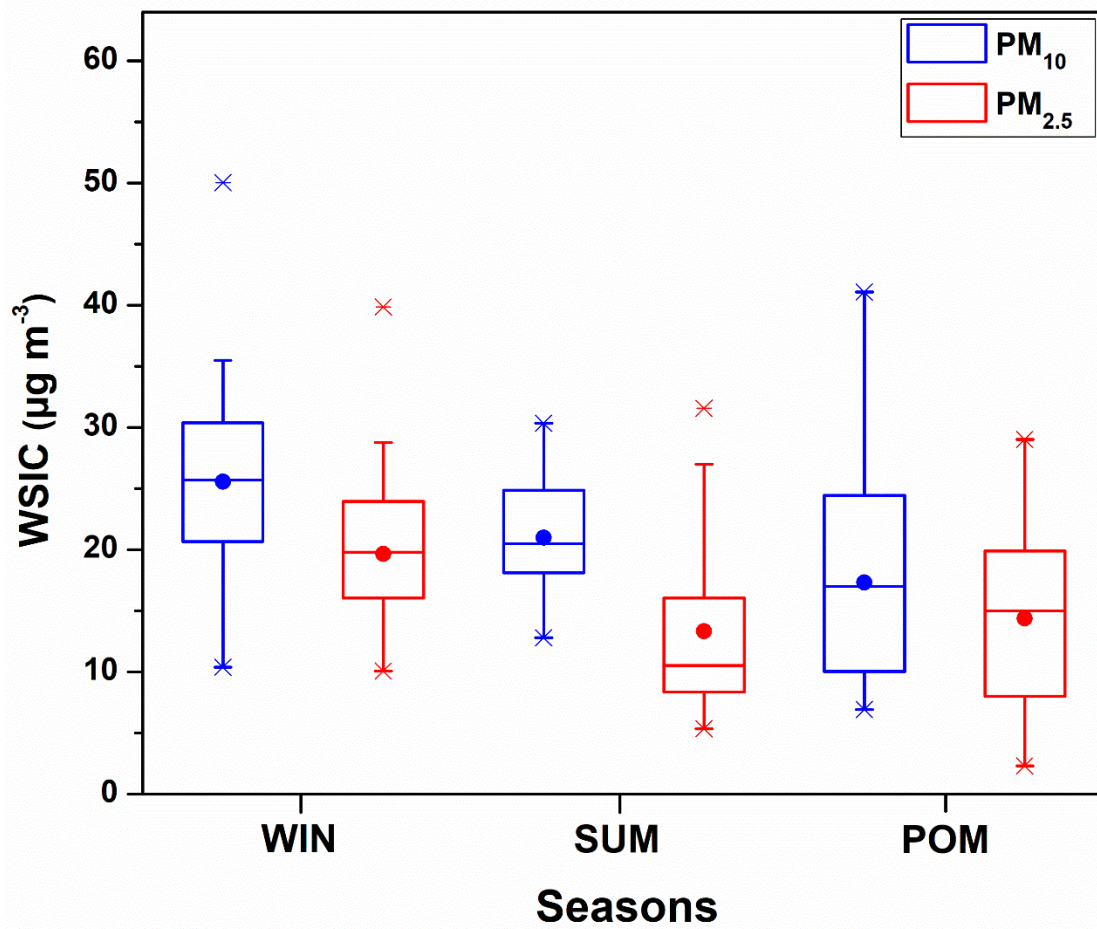


Fig. 4. Seasonal variability of water soluble ionic composition of PM₁₀ and PM_{2.5} during the study period at Goa.

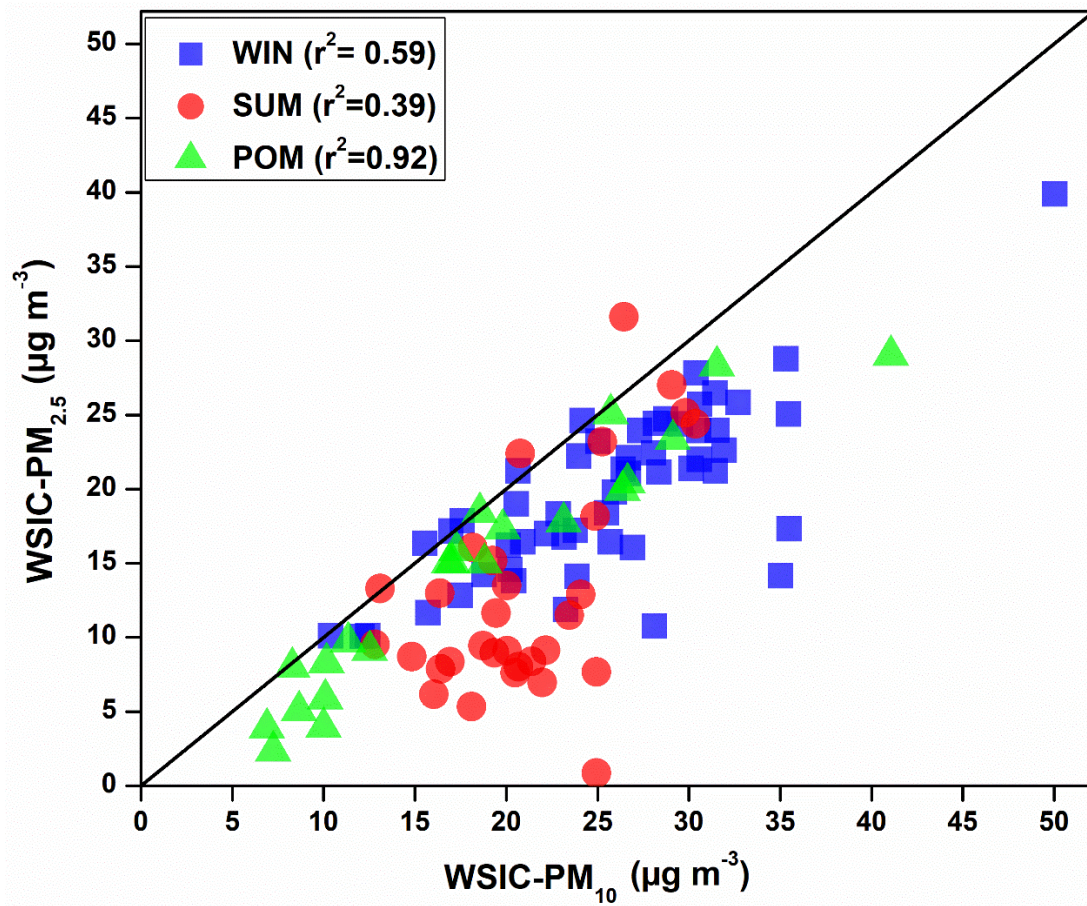
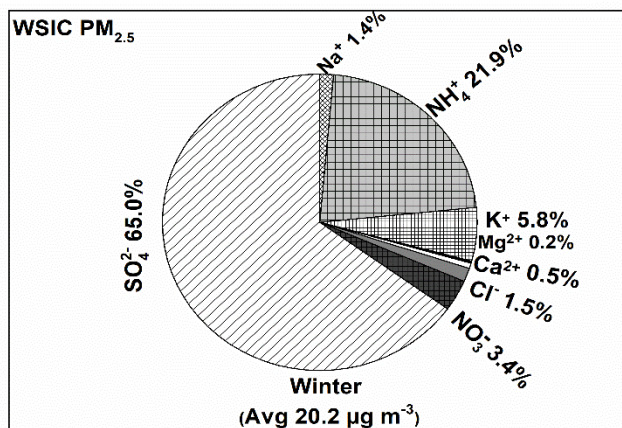
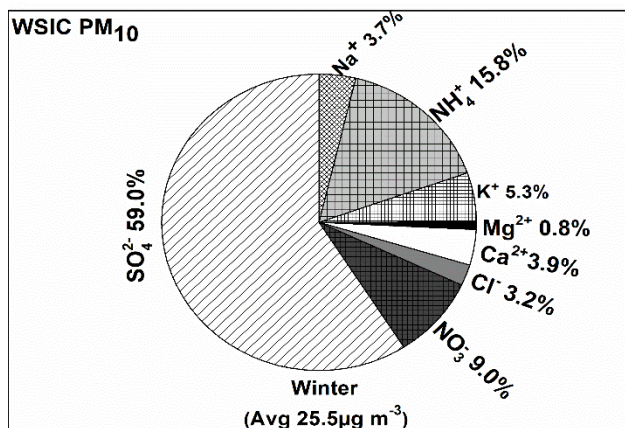
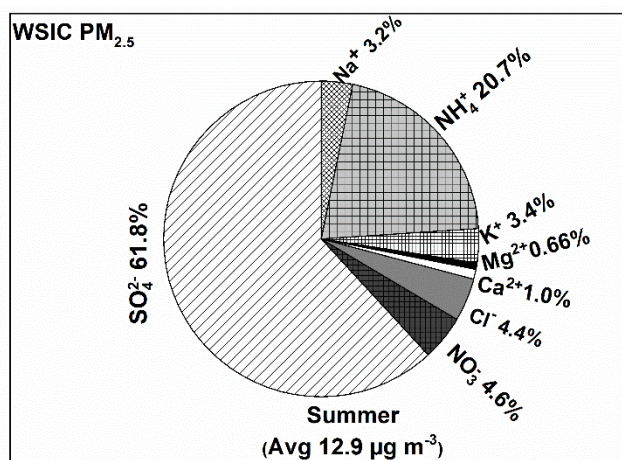
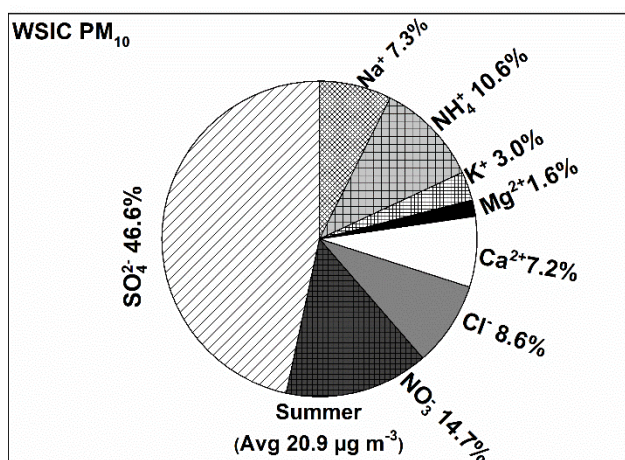


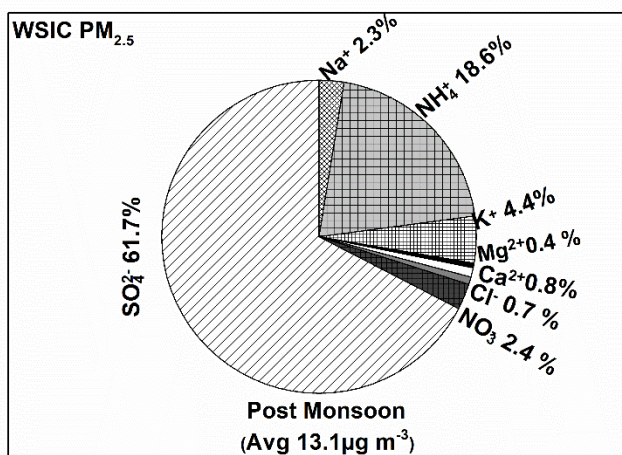
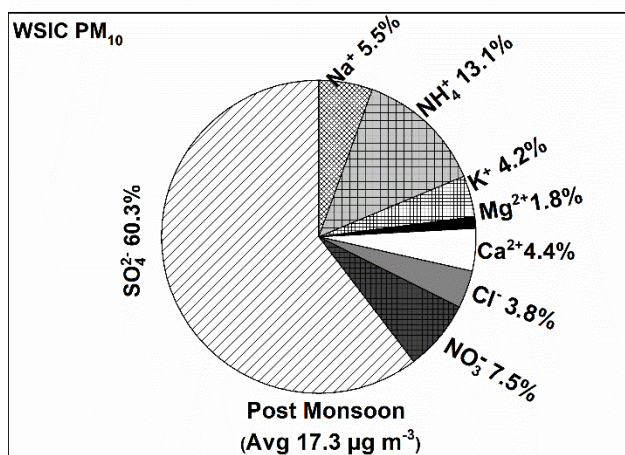
Fig.5: Scatter plot among PM_{2.5}-WSIC and PM₁₀-WSIC, showing relative contribution of WSIC in PM_{2.5} to PM₁₀ WSIC



(a)



(b)



(c)

Fig. 6. Pie chart showing relative contribution of individual ionic species to the total WSIC in PM_{10} and $\text{PM}_{2.5}$ during (a) winter, (b) summer and (c) post monsoon (see text for season description).

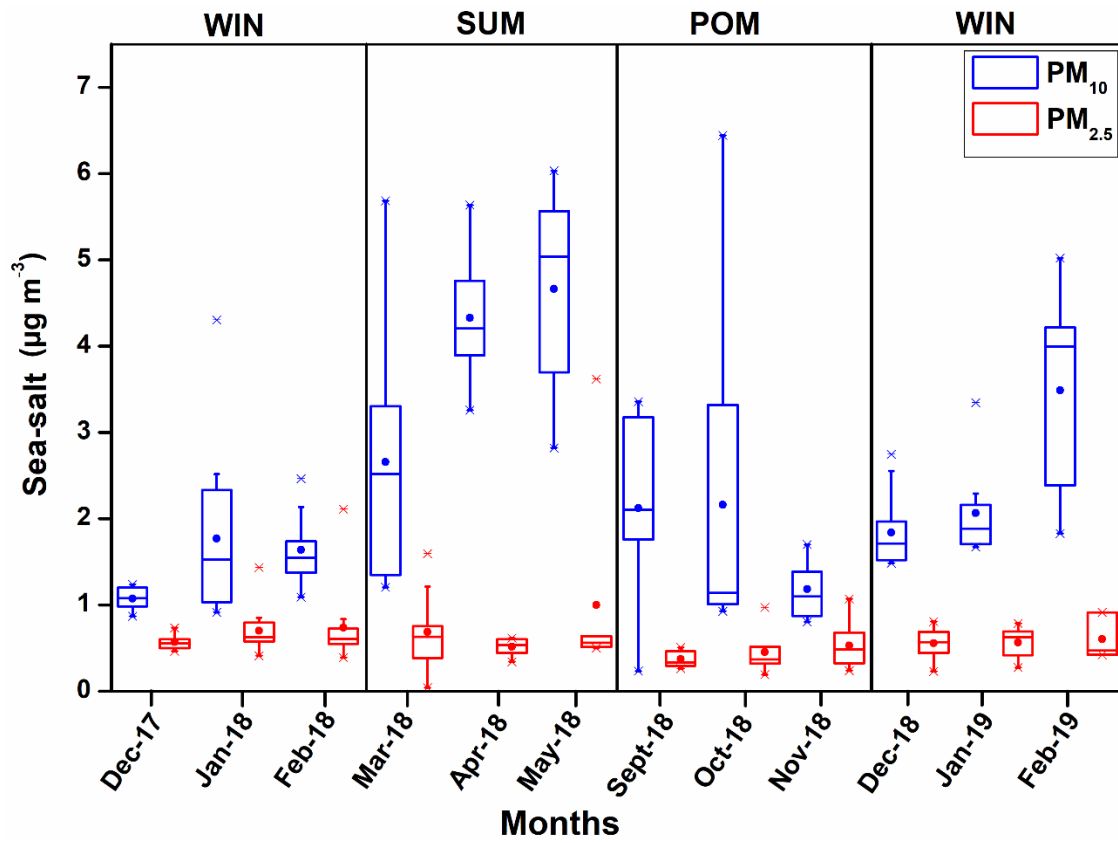


Fig. 7: Box-whisker plots representing the monthly mean (solid line), and different percentile levels (95th, 75th, 25th and 5th) of sea-salt concentrations during the study period. Different seasons are on top x-axis.

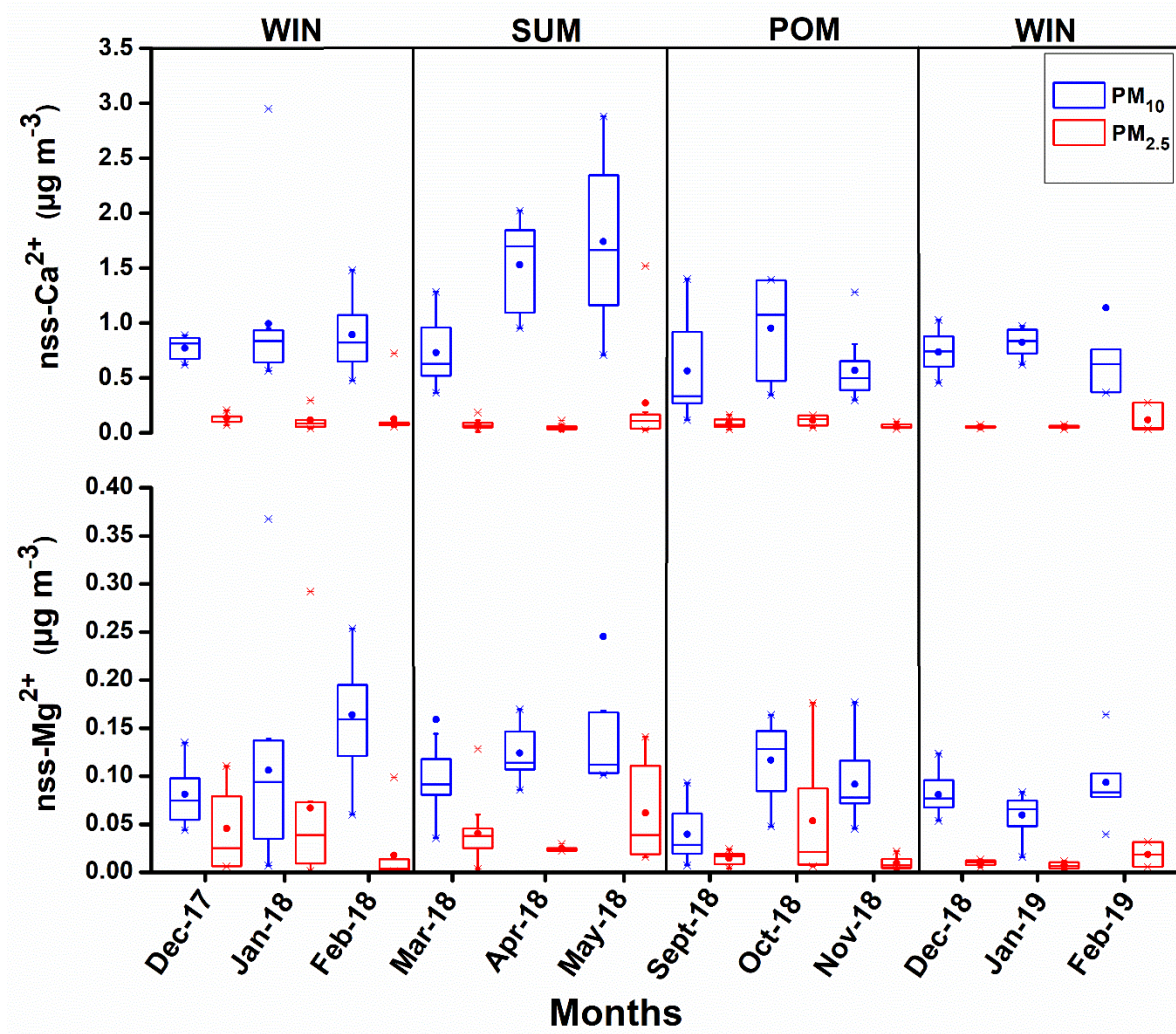


Fig. 8: Box-whisker plots showing monthly variation of nss-Ca^{2+} and nss-Mg^{2+} during the study period.

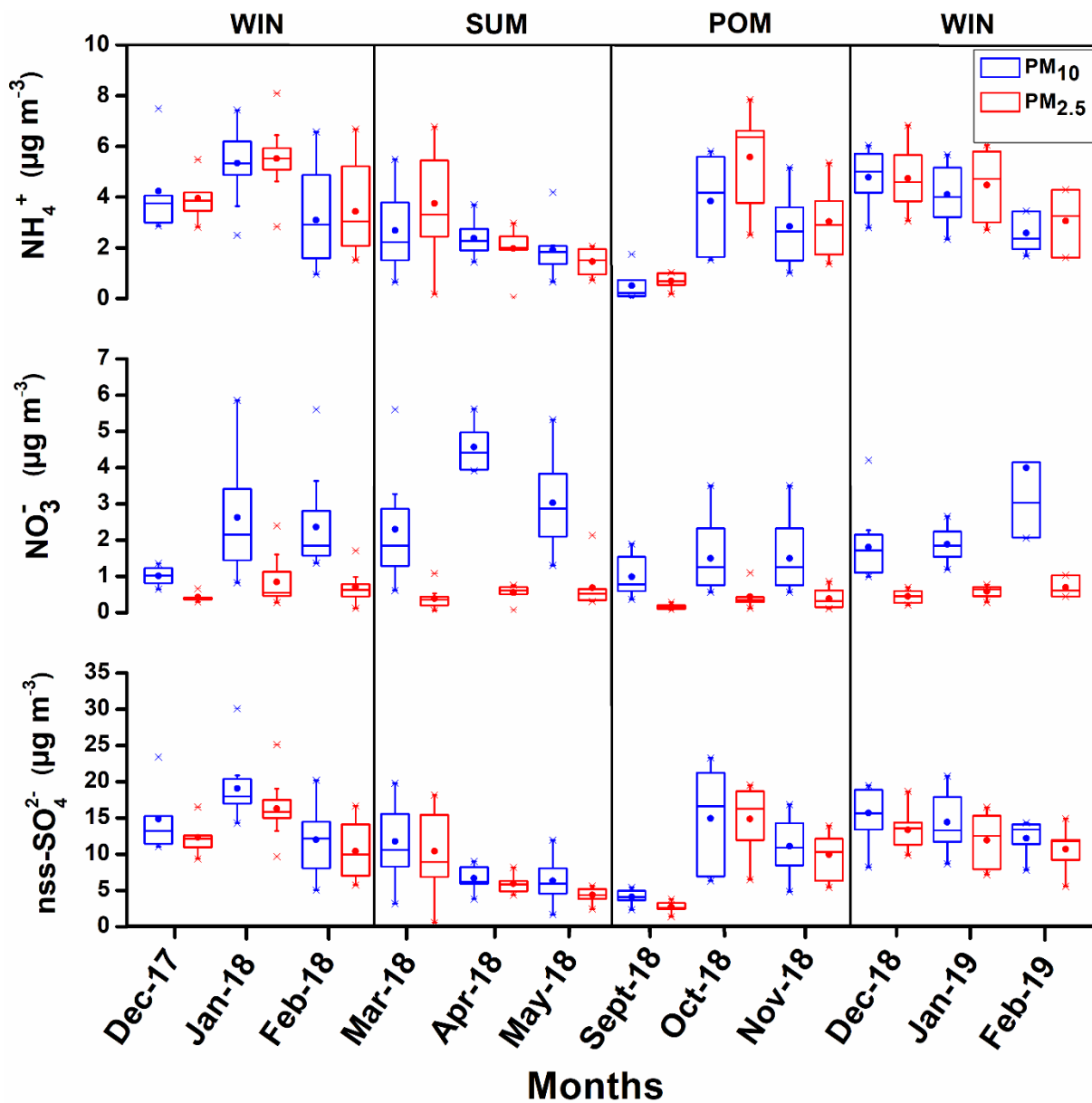


Fig. 9: Box-whisker plots showing monthly variation of secondary ionic species (NH_4^+ , NO_3^- , and nss-SO_4^{2-} ion) in the present study.

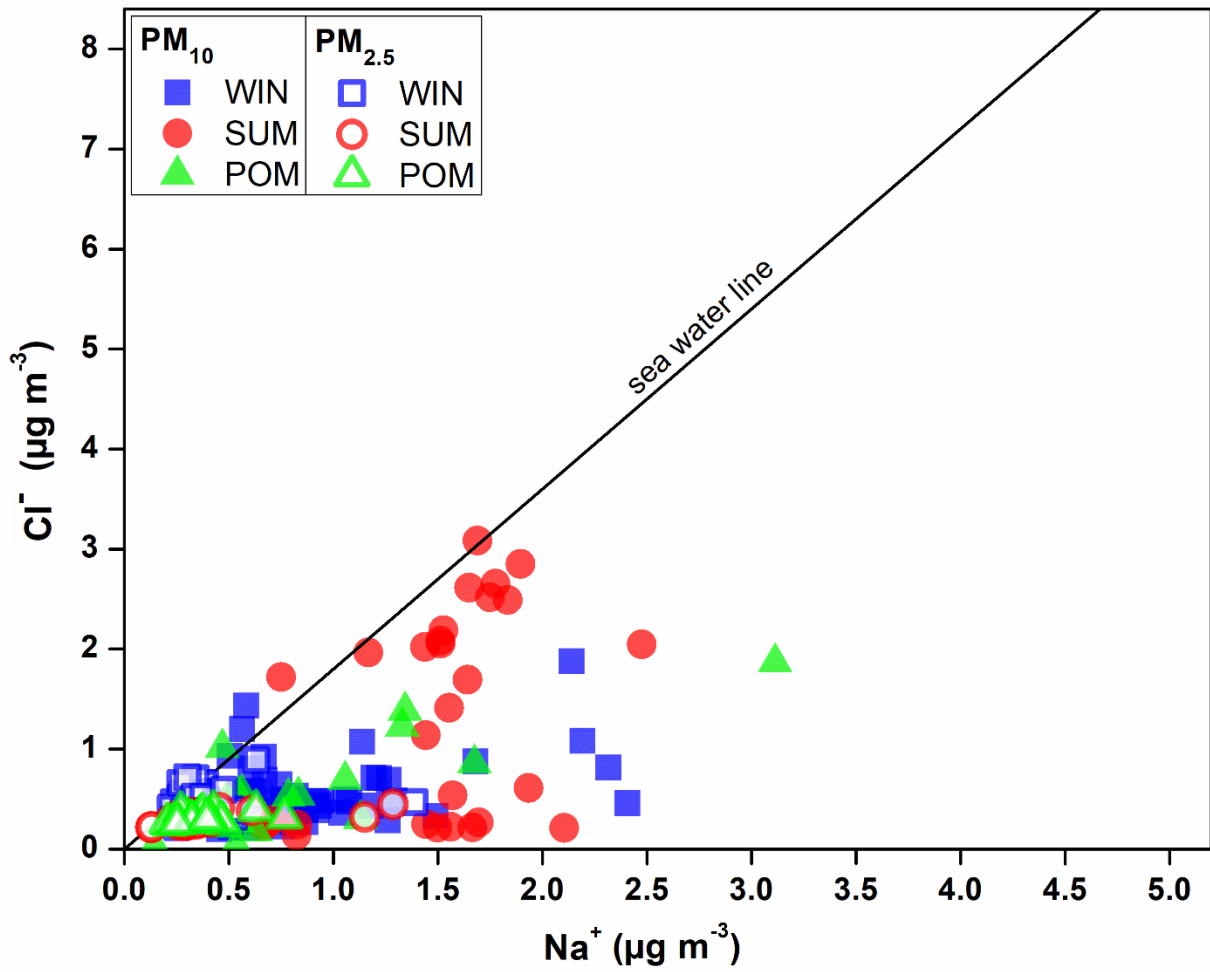


Fig. 10: Scatter plot between Na^+ and Cl^- mass concentration in three seasons at costal sampling station, Goa. The data point falling away from the sea-water line indicate cl-depletion process.

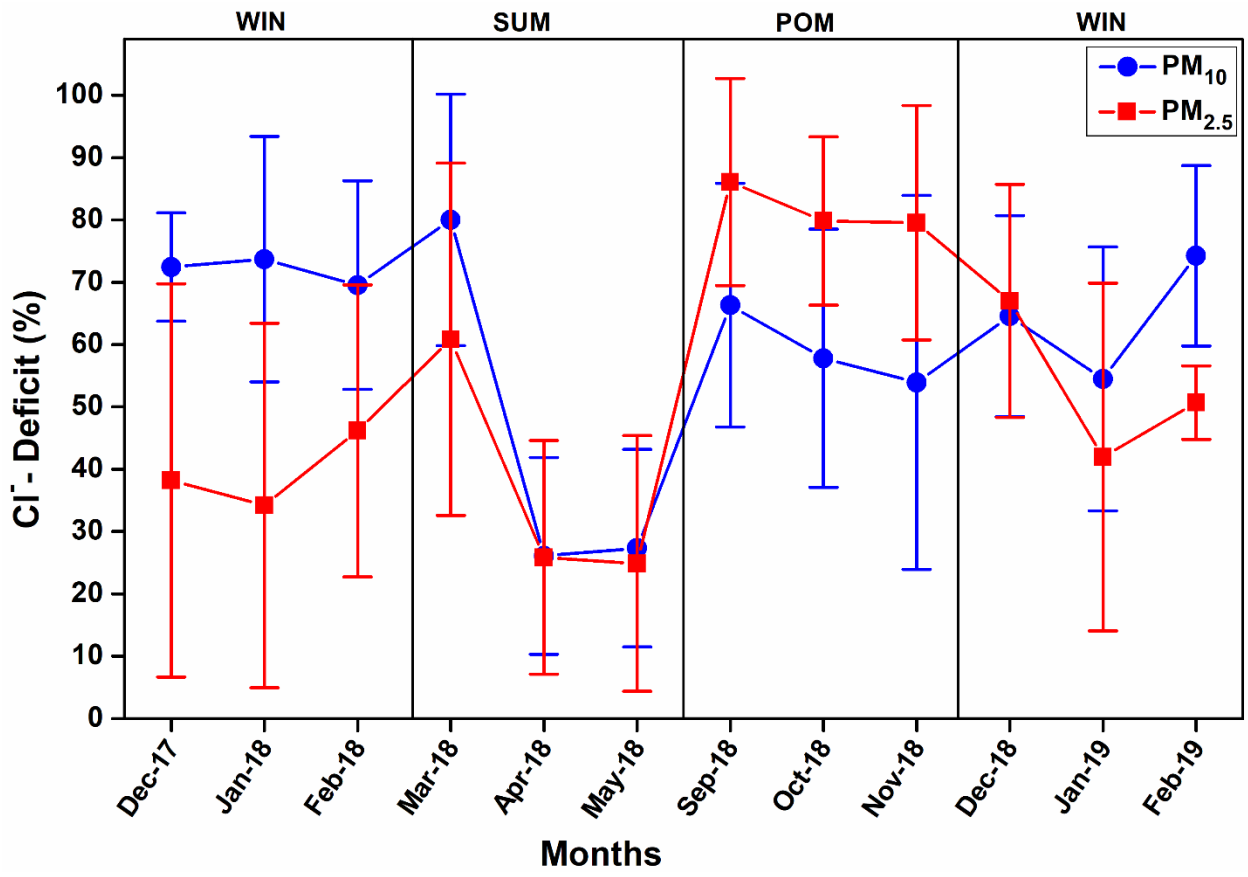


Fig. 11: Variation of monthly average Chloride deficit (%) in PM₁₀ and PM_{2.5} during the study period.

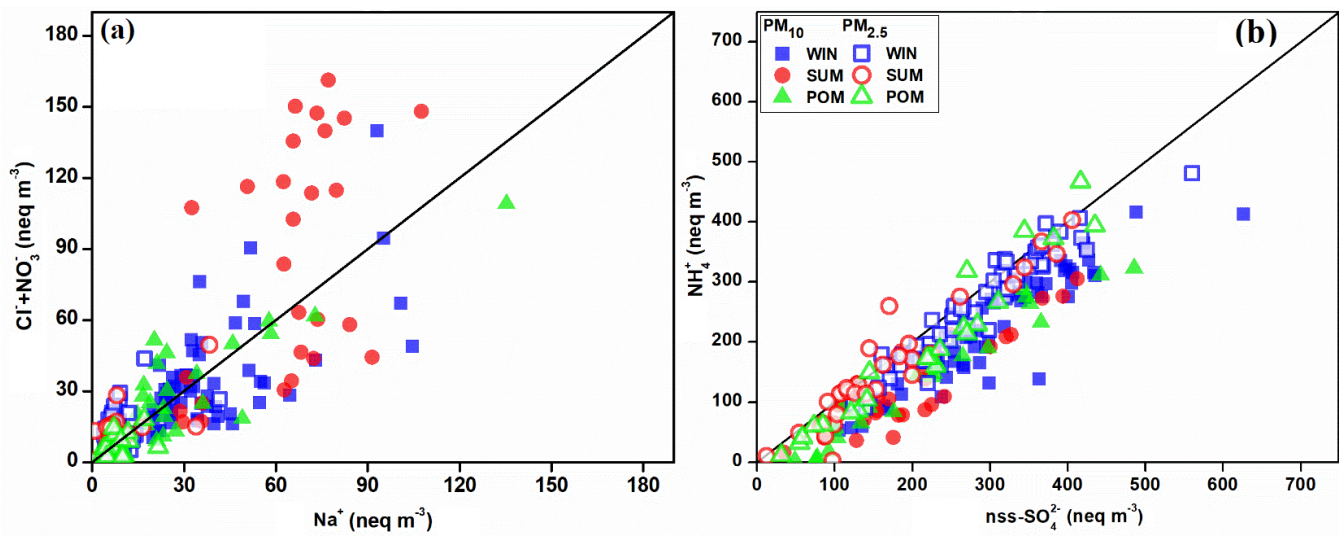


Fig. 12: Scatter plot between (a) $\text{Cl}^- + \text{NO}_3^-$ vs Na^+ ; (b) NH_4^+ vs nss-SO_4^{2-} (in equivalence unit), highlighting the role of secondary species in removal of chloride from sea-salt particle.

Table-1: Details of number of samples, sampling days in each month and type of filter used for PM collection.

Month-Year	Number of samples collected (Both PM₁₀ and PM_{2.5}) (n)	Sampling dates Date of respective month
Dec-17	5	16,20,23,26,30
Jan-18	13	2,4,7,13,15,17,19,21,23,25,27,29
Feb-18	14	2,4,6,8,10,12,14,16,18,20,22,24,26,28
Mar-18	15	2,4,6,9,10,12,14,16,18,20,22,24,26,28,30
Apr-18	8	1,2,3,4,5,6,21,26
May-18	8	1,5,10,13,16,20,22,30
Sep-18	6	13,16,19
Oct-18	7	2,13,16,20,24,27,31
Nov-18	11	4,7,8,9,10,11,12,16,20,23,30
Dec-18	12	4,7,11,14,18,21,24,25,26,27,30,31
Jan-19	8	1,2,3,4,8,15,22,29
Feb-19	5	2,5,10,19,23

*For PM₁₀ total number of samples are 112 (97 Tissuquartz + 15 Cellulose).

* For PM_{2.5} total number of samples are 112 (97 Tissuquartz + 15 Cellulose).

Table 2a and 2b: Table showing seasonal average concentration (in $\mu\text{g m}^{-3}$) of water-soluble PM_{10} and $\text{PM}_{2.5}$ components during the present study respectively.

Components	PM₁₀ (n=112)					
	WINTER (n=55)		SUMMER (n=31)		POST MONSOON (n=24)	
	AM\pmSD	Range	AM\pmSD	Range	AM\pmSD	Range
Na⁺	0.91 \pm 0.47	0.45-2.4	1.45 \pm 0.44	0.66-2.47	0.78 \pm 0.62	0.14-3.11
NH₄⁺	4.15 \pm 1.67	0.95-7.48	2.24 \pm 1.33	0.29-5.40	2.55 \pm 1.82	0.05-5.81
K⁺	1.29 \pm 0.33	0.65-3.16	0.6 \pm 0.38	0.16-1.54	0.7 \pm 0.42	0.14-1.67
Mg²⁺	0.19 \pm 0.09	0.06-0.55	0.31 \pm 0.18	0.12-1.2	0.18 \pm 0.09	0.02-0.51
Ca²⁺	0.96 \pm 0.64	0.45-3.79	1.37 \pm 0.72	0.39-2.94	0.7 \pm 0.41	0.12-1.5
Cl⁻	0.54 \pm 0.32	0.19-1.87	1.58 \pm 1.51	0.13-7.21	0.55 \pm 0.43	0.02-1.86
NO₃⁻	2.25 \pm 1.44	0.64-8.67	2.93 \pm 1.51	0.61-5.60	1.16 \pm 0.72	0.36-3.5
SO₄²⁻	15.21 \pm 4.74	5.18-30.38	9.7 \pm 4.52	1.9-20	10.68 \pm 5.94	2.68-24.1
nss- K⁺	0.95 \pm 0.38	0.16-2.71	0.34 \pm 0.26	BD-1.28	0.54 \pm 0.38	BD-1.47
nss- Mg²⁺	0.08 \pm 0.05	BD-0.36	0.14 \pm 0.18	0.03-1.09	0.08 \pm 0.04	0.007-0.17
nss-Ca²⁺	0.93 \pm 0.64	0.36-3.7	1.31 \pm 0.72	0.36-2.88	0.67 \pm 0.4	0.11-0.14
nss-SO₄²⁻	14.98 \pm 4.74	5.06-30.7	9.30 \pm 4.50	1.66-19.79	10.47 \pm 5.9	2.34-23.31
Sea Salt	1.89 \pm 0.87	0.86-5.02	3.73 \pm 1.7	1.2-8.57	1.70 \pm 1.29	0.23-6.44
WSIC	25.5 \pm 6.9	10.4-50.0	21.0 \pm 4.6	12.8-30.4	17.3 \pm 9.1	6.9-41.1
Cl⁻ deficit*	68.2 \pm 14.3	22.96-89.47	56.20 \pm 32.40	6.44-94.2	61.50 \pm 18.80	19.75-96.77

Components	PM _{2.5} (n=112)					
	WINTER (n=55)		SUMMER (n=31)		POST MONSOON (n=24)	
	AM±SD	Range	AM	Range	AM	Range
Na⁺	0.25±0.15	0.11-1.26	0.48±1.25	0.02-7.13	0.26±0.13	0.1-0.65
NH₄⁺	4.37±1.54	1.51-8.08	2.70±1.75	0.04-6.77	3.34±2.14	0.53-7.84
K⁺	1.05±0.31	0.49-2.61	0.47±0.34	0.02-1.37	0.65±0.35	0.08-1.36
Mg²⁺	0.04±0.02	BD-0.19	0.08±0.15	BD-0.89	0.05±0.04	BD-0.23
Ca²⁺	0.1±0.1	0.03-0.72	0.13±0.31	BD-1.78	0.09±0.04	0.03-0.17
Cl⁻	0.26±0.14	0.01-0.78	0.72±2.26	BD-12.75	0.09±0.07	BD-0.22
NO₃⁻	0.64±0.41	0.12-2.39	0.5±0.38	0.05-2.14	0.36±0.26	0.07-1.1
SO₄²⁻	12.78±4.01	5.65-25.26	7.82±4.48	0.56-18.26	10.1±5.2	2.55-19.64
nss- K⁺	1.04±0.31	0.48-2.59	0.45±0.35	0.02-1.36	0.64±0.35	0.07-1.34
nss- Mg²⁺	BD±0.015	BD-0.06	0.02±0.03	BD-0.14	0.02±0.04	BD-0.17
nss-Ca²⁺	0.09±0.09	0.03-0.67	0.11±0.26	BD-1.51	0.08±0.04	0.03-0.16
nss-SO₄²⁻	12.72±4.00	5.55-25.13	7.7±4.52	0.55-18.20	10.03±5.19	2.47-19.51
Sea Salt	0.54±0.27	0.22-2.11	1.44±4.09	0.04-23.25	0.48±0.23	0.19-1.06
WSIC	19.6±5.8	10.1-39.9	12.9±7.3	0.8-31.6	14.4±8.0	2.32-29.0
Cl⁻ deficit	59.10±21.60	1.9-97.24	58.40±22.50	3.08-100	85.80±10.30	66.92-100

*Cl⁻ deficit in %